Response of bed surface patchiness to reductions in sediment supply

Peter A. Nelson,[1] Jeremy G. Venditti,[2] William E. Dietrich,[1] James W. Kirchner,[1,3,4] Hiroshi Ikeda,[5] Fujiko Iseya,[6] and Leonard S. Sklar[7]

[1] River beds are often arranged into patches of similar grain size and sorting. Patches can be distinguished into "free patches," which are zones of sorted material that move freely, such as bed load sheets; "forced patches," which are areas of sorting forced by topographic controls; and "fixed patches" of bed material rendered immobile through localized coarsening that remain fairly persistent through time. Two sets of flume experiments (one using bimodal, sand-rich sediment and the other using unimodal, sand-free sediment) are used to explore how fixed and free patches respond to stepwise reductions in sediment supply. At high sediment supply, migrating bed load sheets formed even in unimodal, sand-free sediment, yet grain interactions visibly played a central role in their formation. In both sets of experiments, reductions in supply led to the development of fixed coarse patches, which expanded at the expense of finer, more mobile patches, narrowing the zone of active bed load transport and leading to the eventual disappearance of migrating bed load sheets. Reductions in sediment supply decreased the migration rate of bed load sheets and increased the spacing between successive sheets. One-dimensional morphodynamic models of river channel beds generally are not designed to capture the observed variability, but should be capable of capturing the time-averaged character of the channel. When applied to our experiments, a 1-D morphodynamic model (RTe-bookAgDegNormGravMixPW.xls) predicted the bed load flux well, but overpredicted slope changes and was unable to predict the substantial variability in bed load flux (and load grain size) because of the migration of mobile patches. Our results suggest that (1) the distribution of free and fixed patches is primarily a function of sediment supply, (2) the dynamics of bed load sheets are primarily scaled by sediment supply, (3) channels with reduced sediment supply may inherently be unable to transport sediment uniformly across their width, and (4) cross-stream variability in shear stress and grain size can produce potentially large errors in width-averaged sediment flux calculations.

1. Introduction

[2] The grain size distribution of the surface of channel beds typically displays significant spatial structure. Variations occur at all scales, but once they reach mappable domains they are often referred to as patches or facies of common size distributions [e.g., *Dietrich and Smith*, 1984; *Lisle and Madej*, 1992; *Seal and Paola*, 1995; *Crowder and Diplas*, 1997; *Buffington and Montgomery*, 1999a]. Some patches can be texturally stable for many years (even after considerable bed load flux) and remain in a fixed location in the channel, while other patches may migrate downstream as a distinct grain size varying pulse of sediment (as reviewed by *Dietrich et al.* [2005]). The relatively stable (in space) patches appear to arise from shear stress divergences that are forced by topographic controls, such as bar morphology [e.g., *Mosley and Tindale*, 1985; *Laronne and Duncan*, 1992; *Lisle and Hilton*, 1999] flow obstructions such as large woody debris [e.g., *Buffington and Montgomery*, 1999b; *Haschenburger and Rice*, 2004], or immobile accumulations of cobbles or boulders where patches of fine material can accumulate in wake zones [e.g., *Garcia et al.*, 1999; *Laronne et al.*, 2001; *Yager et al.*, 2005; *Yager*, 2007]. Theoretical prediction of the size distribution and occurrence of these patches, however, remains challenging [e.g.,

[1]Department of Earth and Planetary Science, University of California, Berkeley, California, USA.
[2]Department of Geography, Simon Fraser University, Burnaby, British Columbia, Canada.
[3]Swiss Federal Institute for Forest, Snow, and Landscape Research, Birmensdorf, Switzerland.
[4]Department of Environmental Sciences, Swiss Federal Institute of Technology, Zurich, Switzerland.
[5]Environmental Research Center, Tsukuba University, Tokyo, Japan.
[6]Department of Commercial Science, Jobu University, Gumma, Japan.
[7]Department of Geosciences, San Francisco State University, San Francisco, California, USA.

Parker and Andrews, 1985; *Bridge*, 1992; *Lisle et al.*, 2000; *Sun et al.*, 2001a, 2001b; *Julien and Anthony*, 2002]. In systems with decreasing sediment supply, spatially persistent zones of coarse sediment can emerge as a consequence of weaker topographic influences such as grain interactions and general coarsening [*Dietrich et al.*, 1989; *Lisle et al.*, 1993]. Downstream migrating zones of distinct clustering of sediment sizes may organize into thin mappable features referred to as bed load sheets [*Whiting et al.*, 1988]. These features develop from interactions between coarse and fine grains [*Whiting et al.*, 1988; *Dietrich et al.*, 1989; *Tsujimoto*, 1990; *Seminara et al.*, 1996; *Whiting*, 1996]. Following the terminology proposed for bar types [e.g., *Seminara*, 1998], we refer to these end-member types of patches as "forced patches" (spatially persistent associated with strong topographic controls), "fixed patches" (spatially persistent because of weak topographic influences and coarsening), and "free patches" (migrating patches, typically bed load sheets in gravel bed rivers) [*Nelson et al.*, 2005]. The occurrence, distribution and dynamics of these patch types have not been systematically mapped.

[3] Field and flume studies suggest that sediment supply and bed texture are dynamically linked. *Dietrich et al.* [1989] proposed that surface armoring depends on sediment supply. They imposed stepwise reductions in sediment supply to a flume with constant water discharge and observed the expansion of coarse, inactive zones on the channel bed. *Lisle et al.* [1993] used the same flume with a much larger width-to-depth ratio to develop alternate bars. Reductions of sediment supply to this channel caused it to incise, the bars became stationary and emerged, and coarse areas of the channel bed expanded while the zone of active bed load transport narrowed. *Buffington and Montgomery* [1999c] used these and other flume data to show that it may be possible to estimate the quantity of sediment supplied to a reach by comparing the grain size of the bed surface to a theoretically competent grain size. *Kinerson*'s [1990] survey of six field sites with varying supply of coarse sediment suggested that the extent of fine patches may correlate with sediment supply. *Clayton and Pitlick* [2008] suggested that an essentially unlimited supply of coarse sediment allowed the Colorado River to maintain an armor layer during flood conditions. It has also been shown that as the supply of fine material is reduced, armor patches and gravel jams can develop [*Gran et al.*, 2006], and elimination of sediment supply can lead to distinct fixed grain arrangements that substantially alter effective bed roughness [*Church et al.*, 1998; *Hassan and Church*, 2000]. Patches of fine sediment may act as major sources of bed load when hydraulic conditions only allow for partial mobility [*Laronne et al.*, 2001]. *Yager*'s [2007] field study of patches of fine material in a steep mountain channel suggested that their area and thickness should shrink and swell with changes in sediment supply.

[4] All commonly used mixed grain size bed load transport equations [e.g., *Parker and Klingeman*, 1982; *Parker*, 1990; *Wilcock and Crowe*, 2003] are effectively zero dimensional (i.e., no spatial or time components) and do not specifically deal with the effects of patchiness. Sediment flux predictions based on average channel attributes (e.g., depth and mean slope) and spatially averaged grain size distributions are unlikely to be accurate where streambeds

are spatially patchy [*Paola and Seal*, 1995; *Seal and Paola*, 1995; *Ferguson*, 2003; *Chen and Stone*, 2008]. For the case of steep, coarse-bedded channels where patchy finer sediment passes over rarely mobile coarser sediment [e.g., *Garcia et al.*, 1999; *Laronne et al.*, 2001; *Garcia et al.*, 2007], *Yager et al.* [2007] show that bed load transport estimates can be greatly improved by accounting for drag loss over boulders when estimating the effective boundary shear stress, and by applying bed load transport equations only to the portion of the bed that is covered with mobile finer sediment. In these systems, the interconnectedness of fine patches and patch-to-patch transport may be of primary importance under low-stress conditions [*Laronne et al.*, 2001; *Yager et al.*, 2005; *Gran et al.*, 2006]. Discrete particle models that solve the equations of motion for individual sediment grains [e.g., *Schmeeckle and Nelson*, 2003] or that model particle motion with step and exchange rules [e.g., *MacVicar et al.*, 2006] may eventually be able to incorporate and predict patchiness. Thus far, most work has focused mainly on forced patches and their consequences for sediment transport; however, the combined influence of fixed and free patches on bed load transport has not been explicitly explored.

[5] Free patches may be the most active portion of channel, especially if the forced patches are composed of sizes that rarely move. Bed load sheets appear to be the most common occurrence of free patches in the field [*Gustavson*, 1978; *Whiting et al.*, 1988; *Ashmore*, 1991a, 1991b; *Ashworth et al.*, 1992a, 1992b; *Dinehart*, 1992; *Bunte et al.*, 2004] and in flumes during mixed grain size bed load transport [*Iseya and Ikeda*, 1987; *Kuhnle and Southard*, 1988; *Arnott and Hand*, 1989; *Dietrich et al.*, 1989; *Wilcock*, 1992; *Bennett and Bridge*, 1995; *Pender and Shvidchenko*, 1999; *Mikoš et al.*, 2003; *Kuhnle et al.*, 2006; *Lunt and Bridge*, 2007, *Madej et al.*, 2009]. These sorting features have coarse-grained fronts with heights of $1-2$ grain diameters and become progressively finer toward their tails. Bed load sheets form and migrate downstream as a consequence of the "catch and mobilize" process, in which large grains are caught in the wakes of other large grains, followed by infilling of their interstices by smaller particles, which can in turn smooth out hydraulic wakes causing large particles to be remobilized [*Whiting et al.*, 1988]. The sorting patterns across free patches suggest that they pose abrupt changes in roughness and turbulence structure [*Antonia and Luxton*, 1971, 1972; *Best*, 1996]. *Seminara et al.* [1996] proposed that the stress perturbation due to this sorting structure allows for the growth of bed load sheets. *Dietrich et al.* [1989] noted that in response to sediment supply reduction bed load sheets became less frequent and distinct, but did not quantify this observation. Given the growing acknowledgment of and emphasis on the influence of sand on gravel mobility [e.g., *Iseya and Ikeda*, 1987; *Ferguson et al.*, 1989; *Wilcock*, 1998; *Wilcock et al.*, 2001; *Wilcock and Kenworthy*, 2002; *Wilcock and Crowe*, 2003], it is reasonable to ask whether sheets will form in unimodal bed material in which sand is absent. *Gomez et al.* [1989] report "secondary dunes" of a few grain diameters in height and a few tens of grain diameters in length in experiments with gravel between 6 and 64 mm in diameter. They do not, however, report sorting patterns over these features. In general, it is not well known whether bed load sheets can
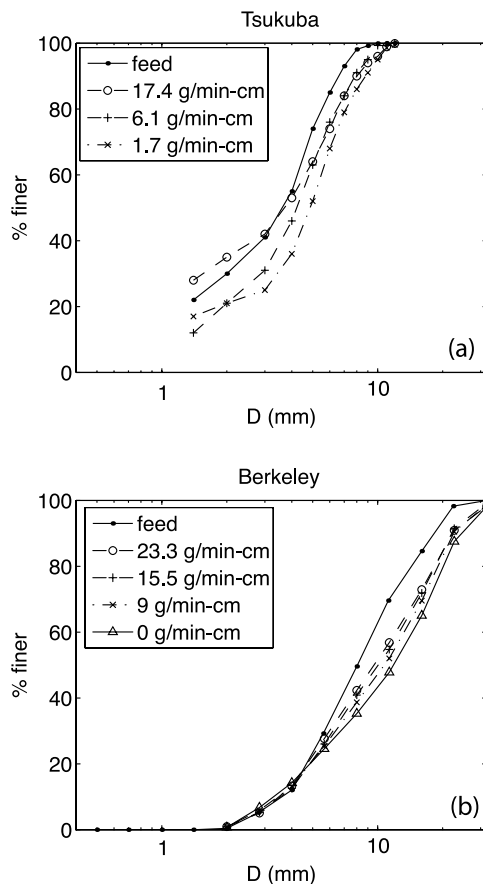
Figure 1. Grain size distributions for the bulk (feed) sediment and bed surface for the (a) Tsukuba and (b) Berkeley experiments.

form in the absence of sand and how sheet characteristics may depend on sediment supply.

[6] In this paper we focus on the relationship between sediment supply and bed surface patchiness and ask the following three questions: (1) what is the relationship between the distribution of free and fixed patches and relative sediment supply; (2) how are the properties of bed load sheets, specifically wavelength and migration rate, influenced by supply; and (3) how does the presence of fixed and free patches influence the prediction of channel slope, grain size, and bed load flux in the simplest case of a straight, low width-to-depth ratio flume. To do this, we revisit the work of *Dietrich et al.* [1989] and present previously unreported data from those experiments. We build upon this work with a new set of experiments conducted with the same general procedure of a stepwise supply reduction under constant water discharge, but in a larger flume using a unimodal, sand-free sediment. We then use data collected in these two sets of experiments to test the full 1-D morphodynamic predictions of bed evolution using the spreadsheet model RTe-bookAgDegNormGravMixPW.xls of G. Parker (1-D sediment transport morphodynamics with applications to rivers and turbidity currents, e-book, 2007, available at http://cee.uiuc.edu/people/parkerg/morphodynamics_e-book.htm). Our analysis shows that as supply is reduced, fixed coarse patches expand at the expense of finer more mobile

patches and result in overall bed coarsening. Large, short-term variations in sediment flux are associated with the migration of free patches, the dynamics of which scale with sediment supply. The Parker (e-book, 2007) model predicts average sediment flux fairly accurately and predicts the corresponding median bed surface grain size and slope to within a maximum difference of 30%. Application of common mixed grain size sediment transport algorithms to our observed shear stress and areally averaged bed surface grain size suggests that for some simple cases, spatial grain size averaging may produce reasonable transport estimates.

2. Methods

[7] The data presented in this paper were collected during two sets of flume experiments. The first were conducted at the University of Tsukuba in Japan in 1987, and have been described in previous publications [*Dietrich et al.*, 1989; *Kirchner et al.*, 1990]. The second set of experiments was conducted at the University of California, Berkeley Richmond Field Station in Richmond, California, United States, in 2005. The procedures for each set of experiments were similar and are described below.

2.1. Tsukuba Experiments

[8] *Dietrich et al.* [1989] progressively reduced the sediment supply to a small (7.5 m long, 0.3 m wide) flume, holding the water discharge (0.6 l/s cm), flume slope (0.0046), and bulk (sediment feed) grain size distribution constant. The width-to-depth ratio was maintained at ~3 in order to suppress development of any channel topography and maintain a simple "one-dimensional" system. The water surface slope, bed slope, and bed surface texture were allowed to equilibrate to the imposed water discharge and sediment supply rate. Sediment was fed into the upstream end of the flume by hand or conveyor belt, and bed load discharged from the end of the flume was collected at 5-min intervals, weighed, and sieved. The water surface and bed surface slopes were measured every 6 min from point gage readings taken at 1-m intervals along the flume centerline. When equilibrium was achieved, that is, when the water surface slope stabilized and the rate and size distribution of bed load transported out the end of the flume matched those of the sediment feed, the run was halted. Each run lasted 6–8 hours, and these procedures were repeated for two reductions in feed rate. The sediment feed was composed of a bimodal sand-gravel mixture of diameter ranging from 1 to 12 mm and with a median grain size (D50) of 3.6 mm (Figure 1a). The initial bed median grain size due to just wetting (i.e., flow without significant transport and particle vibration) was about 4.2 mm. Increased flow and high sediment supply quickly fined the bed to a median grain size the same as the supply. In the three runs, sediment was supplied to the channel at successively reduced rates of 17.4, 6.1, and 1.7 g/min cm. The flow parameters at equilibrium for each run are given in Table 1.

[9] During the experiments, the bed organized itself into 3 or 4 distinct patch types (Figures 2a and 2b and Table 2). Patches were classified as "congested" (coarse-median grain size D50 = 4.68 mm, geometric standard deviation

Table 1. Hydraulic Conditions for Each Set of Experiments

	Tsukuba			Berkeley			
	Run 1	Run 2	Run 3	Run 5-1	Run 5-2	Run 5-3	Run 5-4
Sediment feed rate (g/min cm)	17.4	6.1	1.7	23.3	15.5	9	0
Water discharge (l/cm s)	0.6	0.6	0.6	2.38	2.38	2.38	2.38
Mean flow depth (cm)	10.2 ± 0.04	10.3 ± 0.02	11.3 ± 0.02	21.8 ± 1.6	22.1 ± 0.9	22.4 ± 1.4	22.8 ± 1.2
Water surface slope × 10^{-3}	5.2 ± 0.2	4.6 ± 0.07	3.5 ± 0.08	4.8 ± 0.08	4.6 ± 0.03	4.0 ± 0.05	3.9 ± 0.05
Bed slope				0.0055	0.0051	0.0048	0.0043
Width-to-depth ratio	2.94	2.91	2.65	3.95	3.90	3.83	3.77
Mean flow velocity (m/s)	0.59	0.58	0.53	1.09	1.08	1.06	1.05
Froude number	0.59	0.58	0.50	0.75	0.73	0.72	0.70
Boundary shear stress (Pa)	5.20 ± 0.21	4.64 ± 0.07	3.88 ± 0.09	10.30 ± 0.78	9.94 ± 0.39	8.85 ± 0.55	8.64 ± 0.48
Boundary shear stress (sidewall corrected) (Pa)	4.89 ± 0.20	4.37 ± 0.07	3.63 ± 0.08	10.14 ± 0.76	9.78 ± 0.38	8.71 ± 0.54	8.50 ± 0.46
$D50$ (bed surface) (mm)	3.74	4.26	4.85	9.61	10.05	10.73	11.82
Armoring ratio	1.03	1.17	1.34	1.19	1.25	1.33	1.47
Shields number	0.086	0.067	0.049	0.066	0.061	0.051	0.045
Width of zone of active transport (cm)	–	–	–	61 ± 10	51 ± 12	46 ± 9	–
Length of run (hours)	7.5	7.5	6	16.0	28.9	27.9	20.7

$\sigma = 1.76$), "transitional" ($D50 = 3.63$ mm, $\sigma = 2.16$), "smooth" (fine, $D50 = 2.62$ mm, $\sigma = 2.16$), and "inactive" (coarse zones with no active bed load transport, $D50 = 5.49$ mm, $\sigma = 1.77$) (see *Iseya and Ikeda* [1987] for a discussion of the terms). The grain size distributions for smooth, transitional, and congested facies were measured after the experiment from areas of the bed that were fixed

onto removable boards with cyanoacrylate glue (see *Kirchner et al.* [1990] for details); the grain size distribution for the inactive facies was taken from a grid-by-number Wolman-style [*Wolman*, 1954] pebble count after the lowest feed rate experiment (1.7 g/min cm). This sorting was largely longi-tudinal, forming migrating "congested-smooth" sequences [*Iseya and Ikeda*, 1987] or bed load sheets [*Whiting et al.*,
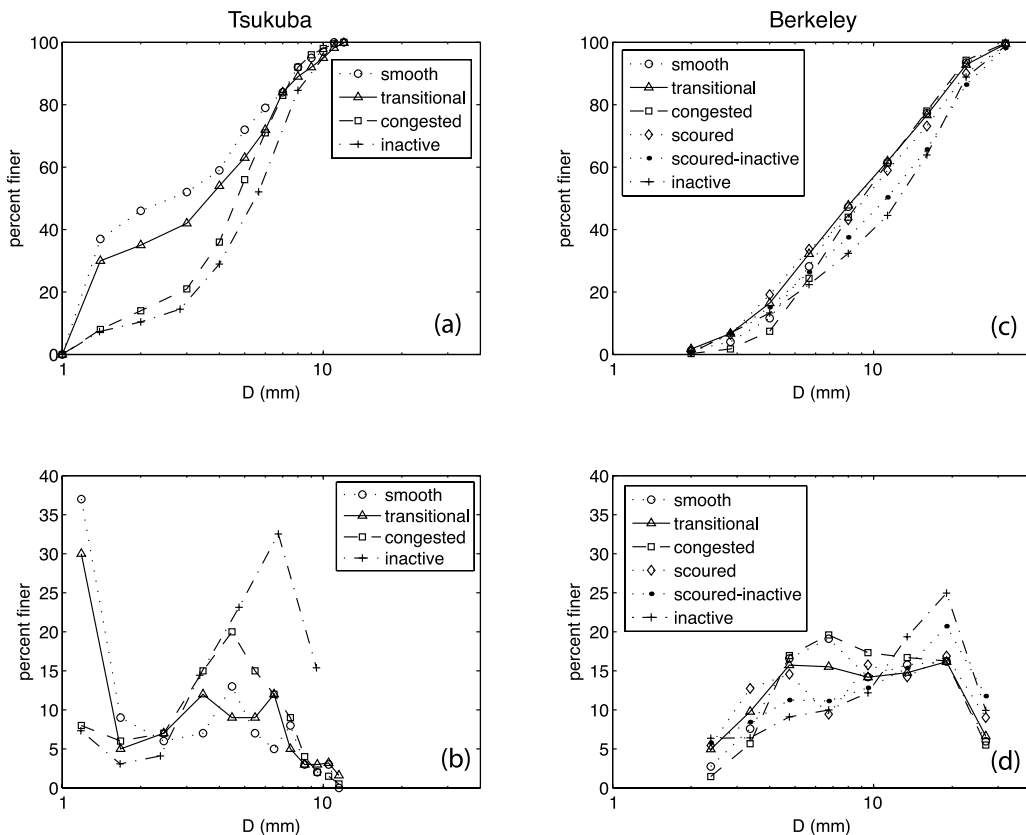

Figure 2. Grain size distributions for patch types mapped during each experiment. (a) Cumulative and (b) probability distributions from the Tsukuba experiments; (c) cumulative and (d) probability distributions from the Berkeley experiments.

Table 2. Grain Size Characteristics of Patch Types Mapped in the Berkeley and Tsukuba Experiments[a]

Patch Type	$D50$ (mm)	σ
Tsukuba		
Smooth	2.62	2.16
Transitional	3.63	2.16
Congested	4.68	1.76
Inactive	5.49	1.77
Berkeley		
Smooth	8.54	1.88
Transitional	8.46	1.96
Congested	9.02	1.81
Scoured	9.3	2.05
Scoured-inactive	11.21	2.05
Inactive	12.47	2.02

[a]Median grain size $D50$ and geometric standard deviation σ.

1988], and during the run the along-flume location of the congested heads of downstream migrating bed load sheets was recorded at 1–2 min intervals. After each run, the entire bed was mapped into these patch types. These patch distributions were used to obtain an area-weighted average grain size distribution for the entire bed surface (Figure 1a). We use this area-weighted size as a metric of surface response although its distribution does not actually occur at any particular location on the channel bed.

2.2. Berkeley Experiments

[10] We performed a similar set of experiments at UC Berkeley's Richmond Field Station (RFS) in Richmond, California. The Berkeley flume is a 28 m long, 0.86 m wide channel. As in the Tsukuba experiments, the width-to-depth ratio was narrow (~4) to suppress the development of bed topography. In these experiments, we performed three stepwise reductions in sediment supply while maintaining a constant water discharge (2.38 l/s cm), flume slope (0.005) and sediment feed grain size distribution. Sediment was fed into the upstream end of the flume using an automatic screw feeder. The downstream end of the flume was equipped with a sediment trap and a load cell that sampled the sediment discharge rate at 60-s intervals. Sediment that exited the flume was diverted to a separate collection basin and samples were taken from this basin at intervals of between 5 and 20 hours and sieved to obtain the average grain size distribution of the transported sediment. The bed surface and water surface elevation were monitored using an ultrasonic water level sensor and an acoustic echo sounder that traversed the flume on a mechanized cart that ran along rails above the flume walls. Water and bed surface elevation were measured at 30–60 min intervals along five longitudinal profiles spaced at 218 mm in the cross-stream direction with the center transect located along the center of the flume. Measurements in the along-channel direction were obtained at an interval of 5 mm. Scans of the bed surface and water surface were performed separately so the echo sounder did not disturb the water surface measurements. The three center profiles were used to calculate average bed and water surface slopes. Between runs, the flume was drained and a range-finding laser attached to the cart was used to obtain a topographic scan of the bed on a 1 × 1 cm grid. A camera was mounted to the cart and between runs the entire bed was photographed from above.

[11] The grain size distribution of the bulk sediment composing the bed and the sediment feed is presented in Figure 1b. We used a unimodal mixture of sand-free gravel ranging in size from 2 to 32 mm with a median grain size of 8 mm. Sediment was fed into the flume at successive rates of 23.3, 15.5, 9 and 0 g/min cm. The run was halted when equilibrium was reached; that is, when the quasi-steady sediment transport rate exiting the flume as measured by the load cell was equal to the sediment feed rate. Each run lasted between 16 and 29 hours. The flow parameters for the experiments are given in Table 1.

[12] During the experiments, the bed was classified (by eye) into patches of similar grain size and sorting, and mapped. As in the Tsukuba experiments, patches ranged from smooth to congested to inactive, although with the unimodal, sand-free bulk mixture, sorting (the geometric standard deviation) played a more critical role in facies discrimination than in the Tsukuba experiments, where the median grain size was sufficient. Bed areas that appeared to have a bimodal grain size distribution were classified as "scoured," since it appeared that the intermediate-sized material had been stripped from the bed, exposing some finer grains. The coarsest areas that experienced little to no sediment transport were classified as inactive. However, some areas of the bed that experienced very little sediment transport were distinguishable from the inactive facies in that they contained a slightly higher percentage of fine material; these were classified as "scoured-inactive" since they resembled a coarser, inactive version of the scoured facies. The grain size distributions of the patch types were later derived by selecting representative photos and performing a digital grain size analysis where a 10 × 10 grid with a spacing of 5 cm was overlain on the center of the channel in the photo and at each point the intermediate axis of the intersecting grain was recorded. Although grain size distributions obtained from photographic analysis will be affected by grain shape and imbrication (see review by *Bunte and Abt* [2001]), these effects can be minimized in a laboratory setting where the overall sediment characteristics are known, and here the photographic method provided both a time-saving technique and a nondestructive visual archive of the entire bed. Figures 2c and 2d present the average grain size distribution for each patch type, and Table 2 summarizes the calculated median grain size ($D50$) and geometric standard deviations (σ) for these distributions. The $D50$ of the congested, smooth, and transitional patch types was between 8.46 and 9.02 mm. The congested and transitional patches could be visually distinguished by their degree of sorting; congested patches were the most well sorted ($\sigma = 1.81$) and transitional patches were relatively poorly sorted ($\sigma = 1.96$). The scoured, scoured-inactive, and inactive patch types each had similar sorting values ($\sigma \approx 2$) and the major difference between them was in the median grain size, the $D50$ for the scoured patches was 9.3 mm while that of the inactive patches was 12.47 mm. Maps were also constructed of the dry bed at the end of each feed reduction. Similar to the Tsukuba experiment, the photographically derived patch grain size distributions were combined with patch areas derived from the maps to obtain an area-weighted average grain size distribution of the entire bed at the end of each run.

Table 3. Input Parameters for Morphodynamic Model[a]

Variable	Variable Abbreviation	Units	Tsukuba			Berkeley			
			Run 1	Run 2	Run 3	Run 5-1	Run 5-2	Run 5-3	Run 5-4
Sediment feed rate	$qbTf$	$m^2/s \times 10^{-6}$	10.90	3.82	1.07	14.63	9.75	4.88	0
Water discharge	q_w	m^2/s	0.06	0.06	0.06	0.238	0.238	0.238	0.238
Intermittency	I		1	1	1	1	1	1	1
Initial bed slope[b]	$Sfbl$		0.0046	–	–	0.0051	–	–	–
Reach length	L_r	m	7.5	7.5	7.5	30	30	30	30
Time step	dt	days $\times 10^{-5}$	2.6	2.5	1.4	0.12	0.12	0.12	0.12
Number of segments	M		30	30	30	90	90	90	90
Active layer factor[c]	n_a		1	1	1	1	1	1	1
Upwinding coefficient	au		0.75	0.75	0.75	0.75	0.75	0.75	0.75
Output frequency[d]	Mtoprint		2000	3000	3000	120	120	120	120
Output frequency[d]	Mprint		6	6	6	480	868	836	620
Time simulated	Calc time	hours	7.5	10.8	6	16.0	28.9	27.9	20.7

[a]See Parker (e-book, 2007) for details of the model.
[b]Only used in the first run, later runs used the final bed profile from the previous run.
[c]Factor by which surface $D90$ is multiplied to obtain active layer thickness.
[d]Mtoprint is the number of steps until output is recorded; Mprint is the number of printouts after the initial one.

2.3. One-Dimensional Morphodynamic Modeling

[13] One-dimensional morphodynamic models cannot account for lateral bed surface heterogeneity; however, the difference between experimental results where patches are documented and 1-D model predictions can provide an avenue for quantifying the effect of patches on sediment transport and channel characteristics. To facilitate such a comparison, we simulated the Tsukuba and Berkeley experiments with a one-dimensional morphodynamic model, RTe-bookAgDegNormGravMixPW.xls, which is freely available as an Excel (© Microsoft Corp.) spreadsheet accompanying an e-book (Parker, 2007, available at http://cee.uiuc.edu/people/parkerg/morphodynamics_e-book.htm). In order to have greater control over the model output (i.e., to allow us to smoothly incorporate stepwise reductions in sediment supply), we translated the VBA code in the Excel spreadsheet into MATLAB (© Mathworks Inc.) code. The main input parameters to the model include the reach length, the initial grain size distributions of the bed surface, subsurface, and sediment feed, the initial slope, the sediment feed rate, and the water discharge. At each computational node in the modeled reach, the model calculates shear stresses using a normal flow approximation, calculates bed load transport using the surface-based relation of *Parker* [1990] or *Wilcock and Crowe* [2003], and calculates changes in bed surface elevation and grain size using the 1-D Exner equation with the active layer assumption. Here, the Tsukuba experiments (which had a significant sand component) were modeled using the *Wilcock and Crowe* [2003] relation, while the sand-free Berkeley experiments were modeled using both the *Parker* [1990] and *Wilcock and Crowe* [2003] relations. Table 3 provides the input parameters used in the modeling.

3. Results
3.1. Mean Hydraulic Conditions and Bed Characteristics

[14] Table 1 shows the mean hydraulic conditions at the end of each run for both sets of experiments. In the Tsukuba experiments, as the sediment feed rate was reduced from 17.4 to 6.1 and then to 1.7 g/min cm, the water surface slope decreased from 0.0052 to 0.0046 and then to 0.0035

(Figure 3a), and the mean flow depth varied only slightly, ranging from 10.2 to 11.3 cm. These slope reductions along with the relatively constant depth resulted in a decrease in the boundary shear stress during the experiment, from 5.2 Pa under the 17.4 g/min cm feed rate to 3.88 Pa under the lowest feed rate of 1.7 g/min cm (Figure 3b). The slope decrease was accompanied by bed degradation, which was greatest at the upstream end because the downstream elevation of the bed was fixed.

[15] In the Berkeley experiments, the mean depth varied only slightly, increasing from 21.8 cm at the highest feed rate of 23.3 g/min cm, to 22.8 cm at a feed rate of zero. The water surface slope was 0.0048 with the highest sediment feed rate of 23.3 g/min cm and decreased with each feed reduction, ultimately reaching a value of 0.0039 during the zero-feed run. The bed slope exhibited a similar decrease from 0.0055 at the highest feed rate to 0.0043 during the zero-feed run, although both the bed and water surface slope displayed substantial variability throughout the course of the experiment (Figure 4a). These slope reductions decreased the boundary shear stress, which fell from 10.3 Pa at the highest feed rate to 8.64 Pa with zero feed (Figure 4b). As in the Tsukuba experiments, the slope decrease was accompanied by bed degradation that was greatest at the upstream end of the flume.

[16] For each experiment, the shear stress τ_b was calculated as $\tau_b = \rho g h S$ where ρ is the density of water, g is gravitational acceleration, h is mean flow depth, and S is the water surface slope. The uncertainties in the depth and slope measurements (the standard error calculated from the repeated measurements) were propagated through the calculation to estimate shear stress uncertainties. Table 1 also presents sidewall-corrected shear stress (calculated with the *Williams* [1970] method).

[17] Substantial changes in the surface grain size distribution also accompanied the reduced sediment feed. For both experiments, on a flume-averaged basis, the surface coarsened with each supply reduction. Figures 1a and 1b show the area-weighted average surface grain size distributions at the end of each run for each experiment. In the Tsukuba experiment, the average median grain size of the bed surface was 3.74 mm at the highest feed rate of 17.4 g/min cm.
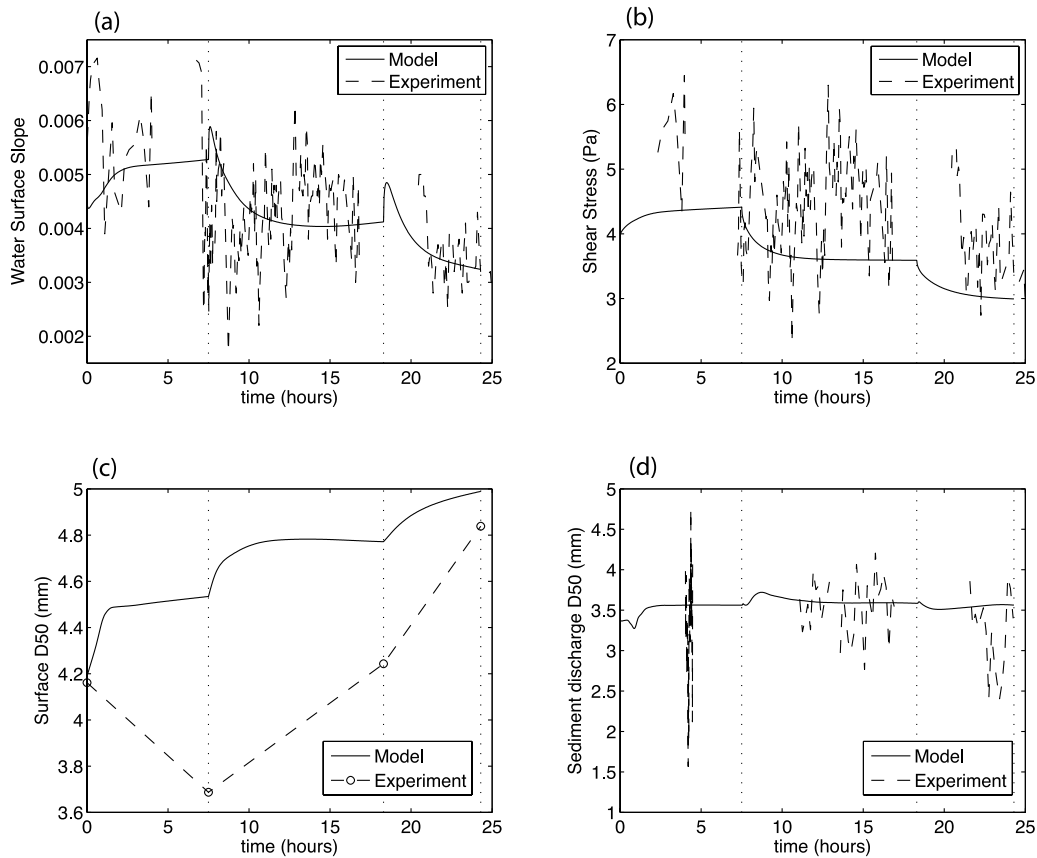
Figure 3. Experimental results and model predictions for the Tsukuba experiments for (a) water surface slope, (b) shear stress, (c) median grain size of the bed surface, and (d) median grain size of the sediment discharge.

After the feed rate was reduced to 6.1 g/min cm, the surface $D50$ increased to 4.26 mm, and after the feed rate was further reduced to 1.7 g/min, the surface coarsened to a $D50$ of 4.85 mm. As noted above, the initial surface grain size before transport was coarser than the load, but with first introduction of the high feed rate the areally averaged channel $D50$ fined to nearly that of the load. Assuming that the $D50$ of the subsurface and that of the sediment feed were similar ($D50$ = 3.65 mm), these average median surface sizes correspond to armoring ratios (surface $D50$/subsurface $D50$) of 1.03, 1.17, and 1.34 for feed rates of 17.4, 6.1, and 1.7 g/min cm, respectively. Similar overall coarsening was observed in the Berkeley experiments (Table 1). Under the highest feed rate of 23.3 g/min cm, the areally weighted surface $D50$ was 9.61 mm. The surface coarsened to a $D50$ of 10.05 mm after the feed rate was reduced to 15.5 g/min cm, then coarsened further to 10.73 mm after the feed rate was reduced to 9 g/min cm, and finally it coarsened to 11.82 mm after an extended period with no feed. When compared with the $D50$ of the feed (8.06 mm), these values correspond to average armoring ratios of 1.19, 1.25, 1.33, and 1.47 respectively.

3.2. Observations of Bed Surface Patchiness

[18] In both the Tsukuba and Berkeley experiments, the bed became organized into patches whose distribution varied with sediment supply. Figures 5 and 6 are maps representing the bed during each experiment under different

sediment feed conditions. In the Tsukuba experiments (Figure 5), as mentioned by *Dietrich et al.* [1989], inactive and congested zones expanded as the sediment supply was reduced. Active transport became confined to a corridor down the center of the channel, the width of which narrowed as sediment supply was reduced. At the lowest sediment transport rate the bed ultimately exhibited a virtually uniform pavement. A map of the bed at the lowest sediment feed rate was not made because of this lack of variability.

[19] Similar results were observed in the Berkeley experiments (Figure 6). As the supply was reduced, coarse inactive zones along the flume walls expanded at the expense of the finer smooth and transitional areas. These coarse patches along the channel edges were not forced by topography, but were fixed as a consequence of coarse grain interactions and near-wall boundary shear stress reduction (and were present to some degree even at the highest load). Sediment transport was primarily confined to a narrow, finer corridor in the center of the channel. The width of this zone of active transport decreased as the sediment supply was reduced (Table 1). Analysis of bed maps indicates that at the highest supply rate of 23.3 g/min cm, the width of this zone of active transport was 61 ± 10 cm (mean ± 1 standard deviation), and it narrowed to 51 ± 12 cm at 15.5 g/min cm, then 46 ± 9 cm at 9 g/min cm. At 0 g/min cm, all bed surface heterogeneity had essentially been eliminated and this zone of active transport effectively disappeared as the
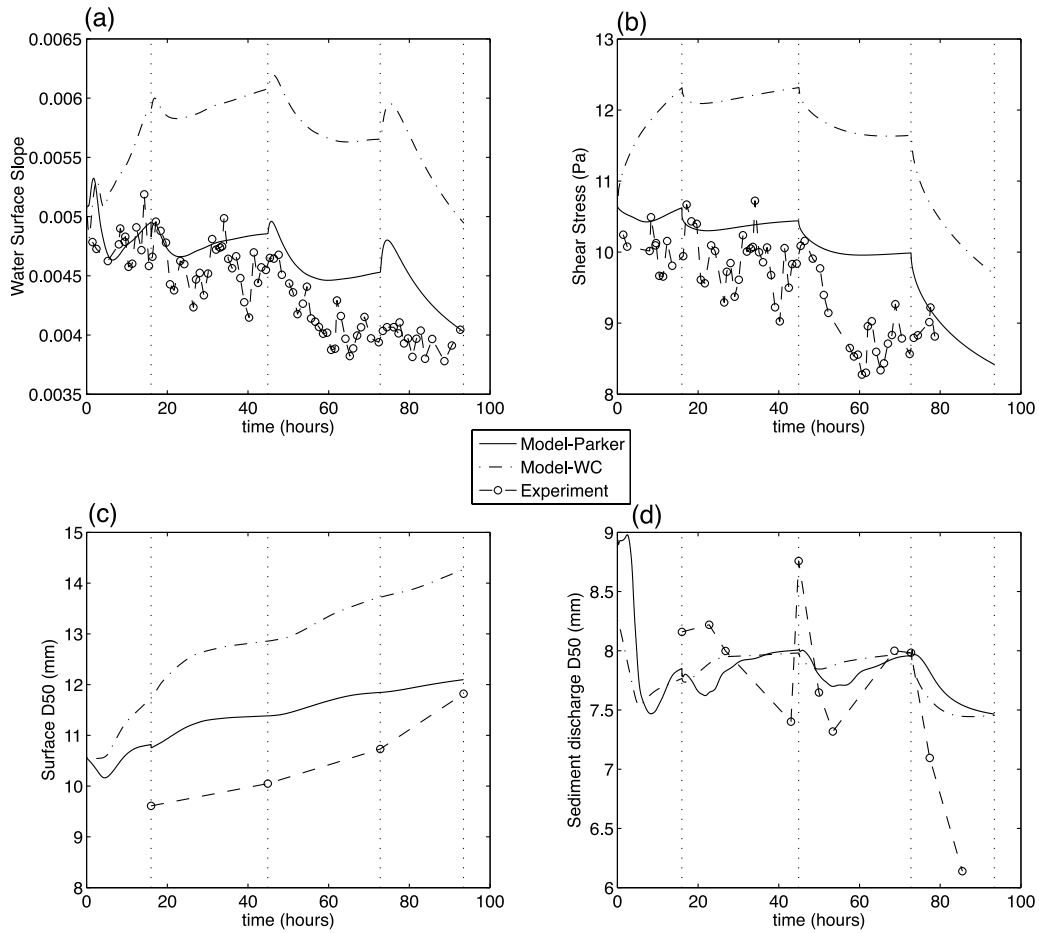
Figure 4. Experimental results and model predictions for the Berkeley experiments for (a) water surface slope, (b) shear stress, (c) areally weighted median grain size of the bed surface, and (d) median grain size of the sediment discharge.

bed became uniformly coarse. The expansion of the area of the coarse patches at the expense of finer patches led to the increase in average $D50$ over the entire bed surface, as documented above.

3.3. Observations of Patch Dynamics

[20] Free (mobile) patches, typically in the form of bed load sheets, were observed in both the Tsukuba and Berke-

ley experiments. These sorting features had coarse-grained fronts with heights of about 2 grain diameters and progressively fined toward their tails. In the Tsukuba experiments, coarse gravel particles became trapped in each other's wakes and accumulated into congested zones, forming the coarse front of bed load sheets. As sand from the tail advanced and began to bury the upstream portion of the sheet head, coarse material at the tail was exhumed. The
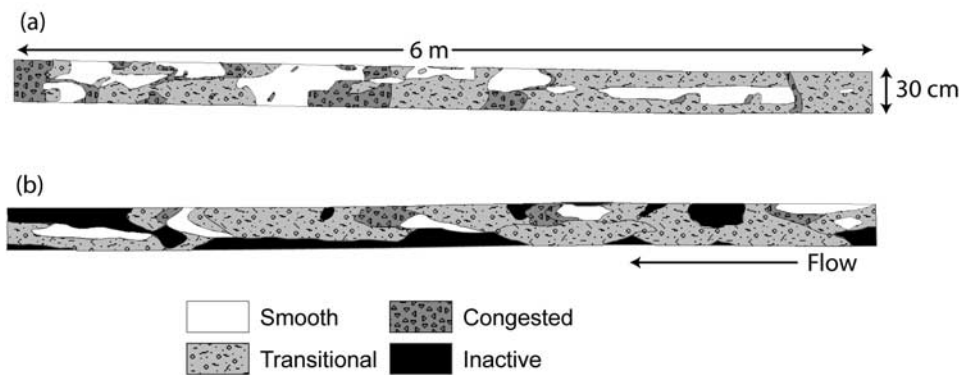

Figure 5. Bed facies map of the Tsukuba experiments at the end of the (a) 17.4 and (b) 6.1 g/min cm sediment feed runs. The 1.7 g/min cm run was not mapped as it was uniformly coarse. See text for description of terms in the legend.
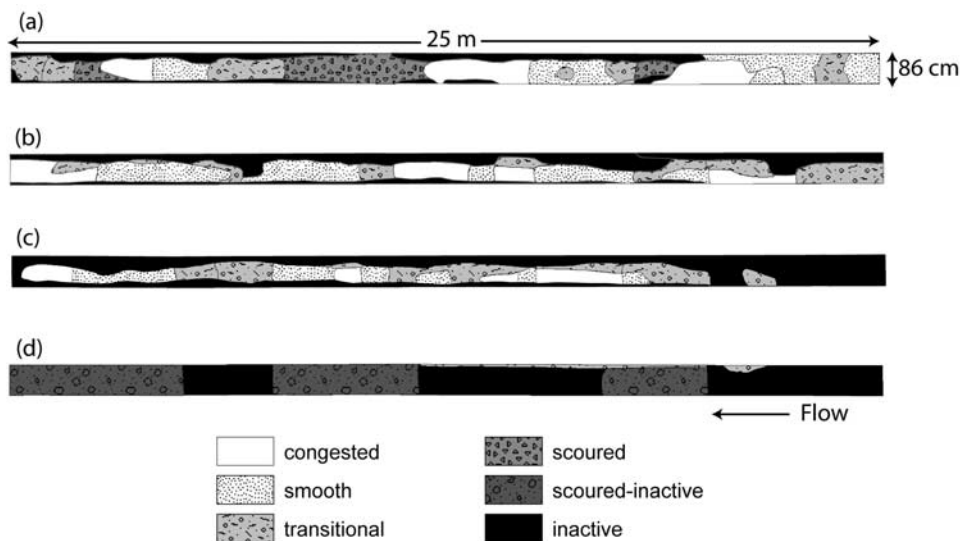
Figure 6. Facies map of the bed of the Berkeley experiments at the end of the (a) 23.3, (b) 15.5, (c) 9, and (d) 0 g/min cm sediment feed runs. See text for description of terms in the legend.

interstices of this coarse material were filled with remnant sand from the tail, which altered the local hydrodynamics and allowed the coarse particles to be remobilized. These remobilized coarse particles advanced to the front of the sheet and were deposited, causing the bed form to migrate. Sheets propagated in a similar manner in the Berkeley experiments even in the absence of sand. In the Berkeley experiments, the front of bed load sheets was composed of relatively well-sorted moderately coarse (8–14 mm) gravel, and these fronts advanced when arriving like-sized material was deposited. As fine (3 mm) gravel from the tail advanced to the front, it exposed coarse material that was remobilized and redeposited at the sheet front. Both of these phenomena illustrate the catch and mobilize process described by *Whiting et al.* [1988]. This process, which takes place over the entire length scale of the bed load sheet, creates the downstream-sorted structure of a bed load sheet and also provides a mechanism for its movement. While this phenomenon had previously only been observed in poorly sorted sand-gravel mixtures, our observations in the sand-free Berkeley experiments suggest that the ratio of coarse to fine grain sizes is probably more important to this process than the mere presence or absence of sand. For grain size segregation to emerge, the coarse front must trap the fines and keep them from passing over it. The range of sizes must be wide enough that the small grains can fit into the interstices between the large grains. For an idealized packing geometry where grains are approximated to be tangent circles, the fine grains can fit into the interstices of the coarse grains with no upstream exposure when the diameter of the coarse grains is four times that of the fine grains. This is largely consistent with the characteristics of bed load sheets presented in Table 4 and suggests a constraint on the range of sizes that can create bed load sheets. Natural bed surfaces are, however, never really geometrically flat, and it appears to take a critical amount of finer sediment deposition (more than one grain) to cause mobilization. The mobilization effect of the fine grains on the coarse grains is likely related to a hydrodynamic smoothing effect that increases the near-bed velocity and drag on the coarse particles [e.g., *Sambrook Smith and Nicholas*, 2005].

[21] In the Tsukuba experiments, the locations of the coarse fronts of bed load sheets were recorded (Figure 7). The lines in Figure 8 represent the motion of individual sheets, so by performing linear regression on each line we can determine the migration rate of each individual sheet and the spacing between successive sheet fronts. Figures 8 and 9 present these data for the duration of the Tsukuba experiments. Although there is substantial variability in the data, it is apparent that, in general, as the supply was reduced the migration rate of sheets decreased and the spacing between sheets increased. Table 4 provides average values of sheet migration rate and spacing computed at the end of each run. Unfortunately, the larger spatial and temporal scale of the Berkeley experiments made acquisition of a similarly detailed data set infeasible. The spacing between sheets, however, was approximated by examining the hand-drawn bed texture maps made during and between runs. These data indicate that, similar to the Tsukuba experiments, the spacing between sheets increased from 6.5 to 9.1 m as the supply was reduced from 23.3 g/min cm to 9 g/min cm (Table 4). Sheets were absent when the feed rate was reduced to 0 g/min cm.

3.4. Effects of Patch Dynamics on Sediment Flux

[22] Figure 10 presents measurements of sediment discharge from both experiments. Several important features are readily apparent in both data sets. First is the decline in the mean transport rate after reductions in sediment supply. As can be inferred from Figures 1, 3c, 4c, 5, and 6, this decline coincided with a general bed coarsening that was a consequence of the expansion of the fixed immobile patches along the flume edges and a reduction of the area occupied by the finer patches. In both experiments, the time-averaged median grain size of the sediment discharged from the flume generally coincided with the median grain size of the feed mixture (Figures 3d and 4d). A second striking feature of the sediment flux time series in Figure 10 is the

Table 4. Characteristics of Bed Load Sheets in This and Other Studies[a]

Reference	H (mm)	L (m)	p (min)	L/H (mean)	L/h	U (mm/sec)	D16 (mm)	D50 (mm)	D84 (mm)	q_s^b (kg/m s)	Shields Number	Conditions
Kuhnle et al. [2006]	7–12	0.07–1.06	0.5–1.15	60	3–4	8–27	1.4	1.82	7.5	0.0647–0.0765	0.066–0.078	Recirculating flume
Bennett and Bridge [1995]	4–13	0.6–1.3	9.5–16.8	56–338	4–13.5	0.7–1.5	1.1–1.2	2.00	3.5–4.2	0.010–0.043	0.04–0.10	Recirculating flume
Wilcock [1992] (MC50)	6–12	1–2					1.8	2.55	6.0	0.018–0.063	0.090	Recirculating flume
Whiting et al. [1988] (Duck Creek)	10–20	0.5–2		83	3.6	1.8–3.5	1.3	4.60	8.7	0.038	0.07–0.11	Field
Whiting et al. [1988] (Muddy Creek)	2–4	0.2–0.6		133	1.3	6–15	0.4	0.90	1.9		0.09–0.18[c]	Field
Bunte et al. [2004]	100–150					10	17	69	166	0–0.05		Field
Kuhnle and Southard [1988]	2–4	0.5–3	5–26	583	24–49	5–10	1.1	3.03	8.0	0.034–0.098	0.036–0.074	Feed flume
Iseya and Ikeda [1987] (Run 6)		1.8			163.6	7.3 (3.6–11.3)	0.3	0.44	2.5	0.0427	0.5[d]	Feed flume
Pender and Shvidchenko [1999]	9–20	2.2–3.5		197	19	0.07–0.18	0.6	3.65	5.9	0.0032–0.0063	0.056	Feed flume
Madej et al. [2009]	~4					10–20	0.4	1	3.2	0.024–0.031	0.015	Feed flume
This study- Tsukuba (Run 1)	5–10	1.4	4.8 (2–15)	197	13.5	9.0	1.1	3.63	5.6	0.0290	0.086	Feed flume
This study- Tsukuba (Run 2)	5–10	1.8	11.5 (2–40)	259	17.6	2.6	1.1	3.63	5.6	0.0102	0.067	Feed flume
This study- Tsukuba (Run 3)	5–10	1.8	23.4 (2–120)	254	15.7	3.5	1.1	3.63	5.6	0.0028	0.049	Feed flume
This study- Berkeley (Run 5-1)	15–30	6.5		217	29.8		4.3	8.06	15.8	0.0388	0.077	Feed flume
This study- Berkeley (Run 5-2)	15–30	9.0		300	40.8		4.3	8.06	15.8	0.0258	0.066	Feed flume
This study- Berkeley (Run 5-3)	15–30	9.1		303	40.5		4.3	8.06	15.8	0.0150	0.057	Feed flume
This study- Berkeley (Run 5-4)							4.3	8.06	15.8	0.0000	0.043	Feed flume

[a]See Notation section for variable definitions.
[b]Sediment transport rate (recirculating flume and field) or sediment feed rate (feed flume).
[c]Whiting et al. [1988] estimate shear stress to be 3–6 times critical for coarse sand.
[d]Shields number for Iseya and Ikeda experiment calculated with the D50 of the feed sediment, all others calculated with the D50 of the bed surface.

tremendous short-term variability in sediment discharge during the experiments. During the high-supply Berkeley experiments the instantaneous flux rates spanned nearly 2 orders of magnitude. The absolute magnitude of these variations in both flumes decreased as the sediment feed rate declined, although the variability relative to the mean flux rate remained relatively constant. In the Tsukuba experiments, sharp increases in sediment flux were primarily the result of increased flux of gravel (rather than sand, see Figure 11a). During short-term periods of high sediment flux up to 85% of the load was gravel, while during periods of lower flux the load could be over 50% sand (Figure 11b). Because bed load sheets in the Tsukuba experiments had gravelly heads and sandy tails, this suggests that high transport rates coincide with the passage of sheet heads and lower transport rates occur either with the passage of sheet tails or between successive sheets.

3.5. One-Dimensional Morphodynamic Modeling

[23] Some of the model predictions for the Tsukuba experiments have already been presented in a previous study [*Dietrich et al.*, 2005] and are summarized here in Figures 3 and 10a. For each feed rate, the surface $D50$ predicted by the model (using the *Wilcock and Crowe* [2003] transport algorithm) is 1.03–1.23 times the observed $D50$; however, the maximum deviation between the model prediction and surface $D50$ is only 0.75 mm, which may be within measurement error (Figure 3c). The water surface slopes at the end of each run predicted by the model are between 0.90 and 1.02 times the measured water surface slopes (Figure 3a). The model consistently underpredicts the average shear stress; modeled stresses are between 0.77 and 0.85 times the measured stresses (Figure 3b). The sediment flux predicted by the model (Figure 10a) does not capture any of the short-term variability due to the passage of bed load sheets as discussed above, but it does equilibrate to the feed rate for each phase of the experiment. The average $D50$ of the sediment discharge predicted by the model at equi-
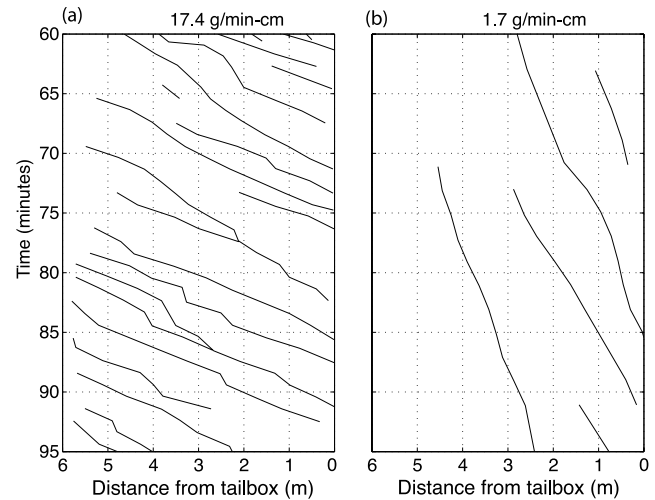

Figure 7. Representative observations of the migration of the coarse fronts of bed load sheets and sediment flux during the Tsukuba experiments at a sediment feed of (a) 17.4 and (b) 1.7 g/min cm.
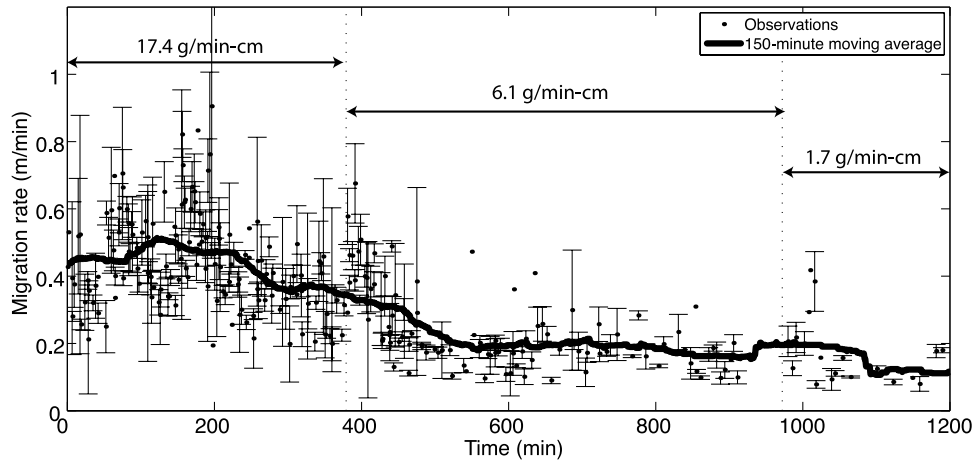
Figure 8. Time series of bed load sheet migration rates during the Tsukuba experiments. Each data point is the migration rate of a single sheet calculated from slope of the time-distance trajectory observations shown in Figure 7. Dotted lines indicate transitions in the sediment feed rate, and the thick line through the data is a 150-min moving average. Error bars indicate 95% confidence intervals of the calculated slopes.

librium is equal to that of the sediment feed and is within the range of the experimental observations (Figure 3d).

[24] When the *Parker* [1990] algorithm is used to model the Berkeley experiments, the model overpredicts the surface grain size at all feed rates (Figure 4c). The predicted surface $D50$ is 1.02 to 1.13 times the observed $D50$ (Figure 4c). As was the case for the Tsukuba experiments, the difference between predicted and observed surface $D50$ decreases with decreasing feed rate and hence bed surface patchiness, suggesting that the model performance improves with decreasing bed surface heterogeneity. The water surface slopes predicted by the model are between 1.00 and 1.12 times the observed slopes (Figure 4a). The model tended to overpredict shear stress, with modeled shear stresses at equilibrium 1.06 to 1.14 times the measured stress (Figure 4b). The model's prediction of the Berkeley

sediment discharge was consistent with the average transport rate in the experiment (Figure 10b). At the end of the computation, however, the model predicted a sediment discharge of 2.5 g/min cm while the measured sediment discharged from the flume was less than 1 g/min cm. Both the predicted and measured $D50$ of the sediment discharge during the feed portions of the experiment tended to equilibrate at the $D50$ of the sediment feed (8 mm), although once the feed was eliminated the measured $D50$ of the sediment discharge decreased more rapidly than that predicted by the model (Figure 4d).

[25] Application of the *Wilcock and Crowe* [2003] algorithm in the 1-D simulation of the Berkeley experiments yielded results in striking disagreement with the experimental observations. Although the model-predicted sediment discharge matched the average transport rate in the exper-
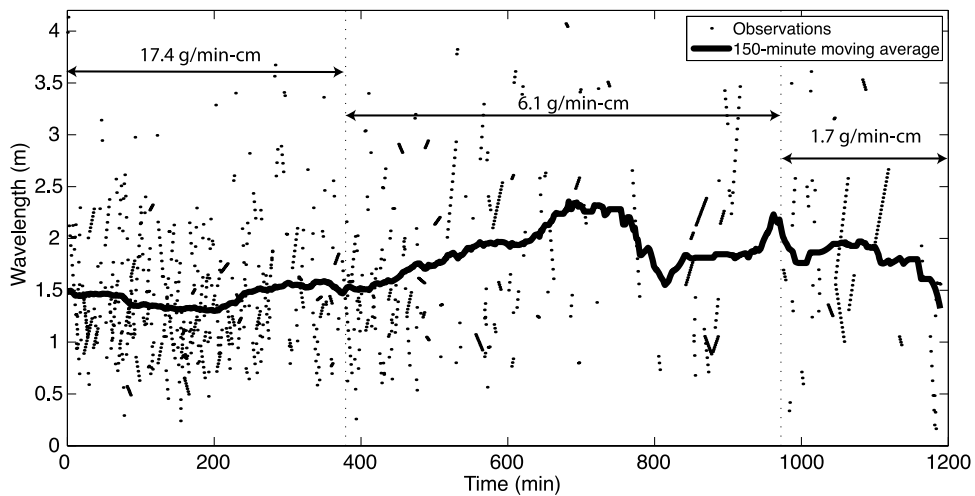

Figure 9. Time series of the spacing between bed load sheets calculated from observations of the type presented in Figure 7 during the Tsukuba experiments. Data points are the distances between adjacent sheets at a given time; dotted lines indicate transitions in the sediment feed rate, and the thick line through the data is a 150-min moving average.
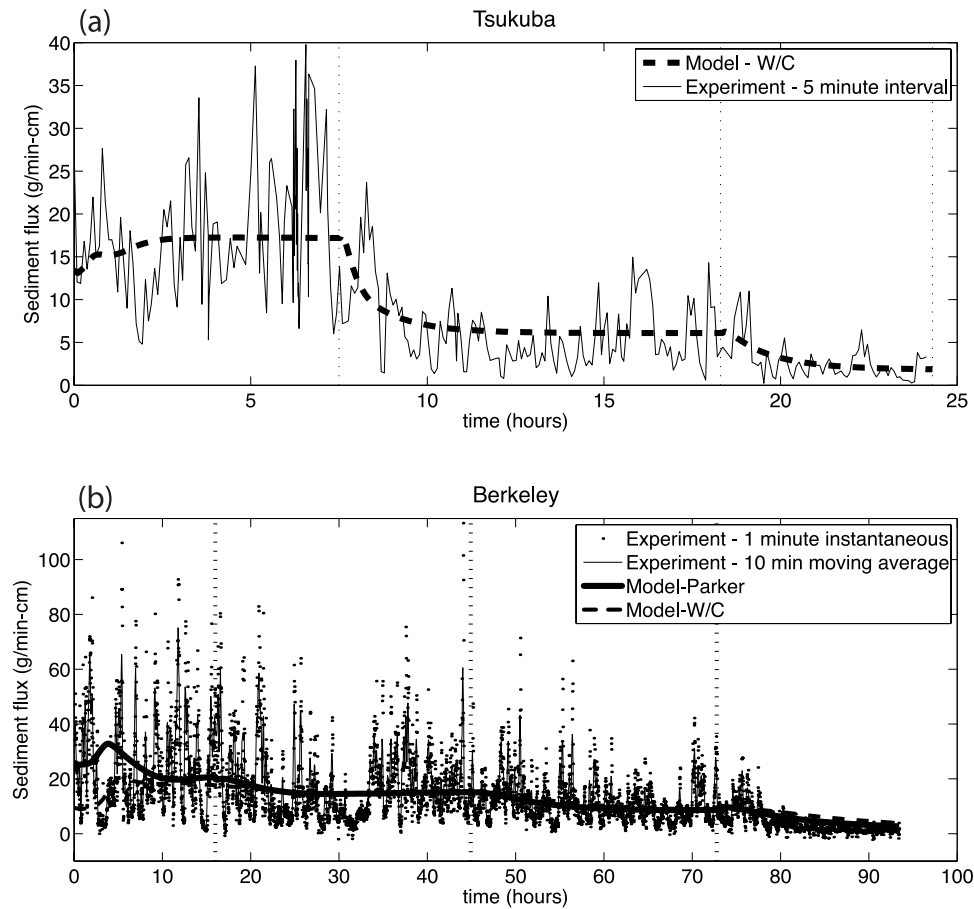
Figure 10. Experimental results and model predictions of sediment flux for the (a) Tsukuba and (b) Berkeley experiments. The sediment feed rates are presented.

iment (Figure 10b), the model achieved that flux rate by predicting steeper slopes, higher shear stresses, and larger surface grain size than were observed (Figure 4).

[26] The transient response of both simulations shows that after a reduction in sediment supply, the model tends to predict a brief increase in the water surface slope, followed by a decrease in slope, then a small gradual slope increase toward an equilibrium value (Figures 3a and 4a). The initial increase in water surface slope occurs because immediately following the supply reduction, the bed of the upstream portion of the channel coarsens, which causes the water surface elevation at the upstream end to increase. This bed coarsening and the accompanying depth increase propagate downstream, but as they do so the upstream portion of the channel begins to scour, which causes the water surface slope to drop. Eventually, the downstream portions of the channel also become scoured and the water surface slope experiences a slight recovery.

4. Discussion

4.1. Sediment Supply and Patch Dynamics

[27] As sediment supply was reduced in the experiments, the resultant surface coarsening did not develop in a uniform manner. Even in the fairly simple (relatively one-dimensional, low width-to-depth ratio, plane bed) conditions of our experiments, the bed displayed remarkable

heterogeneity. As supply was reduced, the bed coarsened through the expansion of coarse, fixed patches that first developed along the flume edges, and a constriction of the finer zone of active transport over which free patches (bed load sheets) were moving. As shown in Figures 8 and 9, the spacing between these sheets and the speed at which they were moving also varied with sediment supply. Only after an extended period of zero feed did the bed become a nearly uniform texture, which in this case was a completely armored, immobile bed.

[28] Table 4 summarizes data from this and several other studies in which the measurements of the characteristics of bed load sheets were made. Bed load sheets are similar to bed forms such as ripples or dunes in that their shape and behavior can described in part by a height (H), wavelength (L), and migration rate (U). It is apparent that the height of bed load sheets scales with the coarse grain diameter, and that they are tens to hundreds of grain diameters in length. Yet, there does not appear to be any consistency in bed load sheet aspect ratio (L/H) or the flow depth to sheet height ratio (h/H). In contrast, dunes have fairly consistent aspect ratios ($L/H = 20$) and scaling with flow depth ($h/H = 5$) in uniform steady flow (see reviews by *Carling* [1999] and *Venditti et al.* [2005]). As is the case for bed load sheets, subaqueous ripples tend to scale with particle diameter ($L \sim 1000\ D$), but they only form in hydraulically smooth flow and consequently are limited to sediment with $D < 0.7$ mm
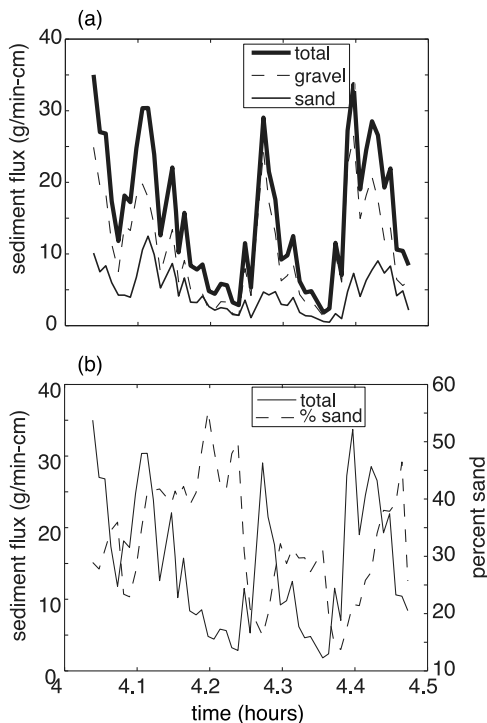
Figure 11. Sediment flux during a portion of the 17.4 g/min cm phase of the Tsukuba experiment. (a) The total rate of sediment transport along with the corresponding rates of sand and gravel transport. (b) The total sediment transport rate and the percentage of the load that was sand.

[*Best*, 1996; *Carling*, 1999; *Venditti et al.*, 2005, and references therein]. Thus, the commonly used methods for scaling bed forms do not apply to bed load sheets. Bed load sheet migration rate decreased and wavelength increased with reductions in sediment supply. This is consistent with the absence of sheets in the low sediment supply channels studied by *Church et al.* [1998] and *Hassan and Church* [2000]. As suggested by *Whiting et al.* [1988], bed load sheets might under certain conditions provide "seeds" for the development of dunes. If flows are competent to carry the load at several times the critical shear stress, it is possible that a threshold sediment supply exists where sheets begin to transform into low-amplitude dunes. Indeed, experiments by *Bennett and Bridge* [1995] seem to suggest this is the case. The earlier work seems to be confirmed by the changes in mixed size bed forms observed by *Kleinhans et al.* [2002], where with increasing flow strength and sediment transport, they observed sand ribbons evolve into barchans and eventually dunes.

[29] The dependence of bed load sheet migration rate on sediment supply can in part be explained through a simple mass balance argument. Sediment flux per unit width, q_s, can be expressed as the product of a bed form's migration rate U, height H, and a shape factor which is normally taken to be constant [*Simons et al.*, 1965]. If the height of a bed form remains constant then an increase in q_s translates directly to an increase in U. A similar mass balance argument can be made to explain why sheet spacing decreases with increased sediment supply. It appears (as suggested by *Whiting et al.* [1988]) that for free patches

such as bed load sheets to form, it is necessary to reach a critical concentration of coarse particles sufficient to create the sheet front (termed "gravel jams" by *Iseya and Ikeda* [1987]). Since more coarse particles become available with a greater sediment supply, the length of the upstream contributing bed area required to develop the sheet front decreases and sheets can form with greater frequency.

[30] This argument depends on the height of the sheet remaining constant (i.e., $1-2$ coarse grain diameters). Studies in which sheets have been documented (Table 4) confirm this assumption, but why should an increase in sediment supply produce greater bed form migration rate rather than increase the bed form height? One important feature that distinguishes sheets from subaqueous dunes and ripples is the strong sorting over the bed form. If all grain sizes are mobile and the grain size distribution is wide enough, the mobilization effect of the fine particles on the coarse ones may provide a limit to the bed form height by mobilizing the coarse particles before they can build a slip face. This continual mobilization would then allow the sheet to migrate downstream more rapidly without appreciable gains in height. This process is likely to be limited to a somewhat intermediate range of sediment supply (relative to channel width) and flow competency, where beyond a certain level sheets may start to frequently merge with each other, forming slip faces and developing dunes. In this framework, then, sediment supply is the primary control on bed load sheet scaling. Hydraulics play a secondary role, in that the flow must be capable of moving the range of grain sizes composing the sheet structure, but must not be so strong as to prevent the initial mutual interactions between coarse particles from forming the sheet front.

4.2. Morphodynamic Predictions in Patchy Channels

[31] The presence of sorted patches on the bed poses potential problems for bed load transport calculations because it becomes necessary to average over the width of the bed to get an input grain size. Given the remarkable heterogeneity and sorting we observed in our experiments (Figures 5 and 6), our uncalibrated application of the Parker (e-book, 2007) one-dimensional morphodynamic model performed quite well, especially for the Berkeley simulation using the *Parker* [1990] algorithm, as some predictions of the median surface grain size, slope, and average sediment flux were nearly within measurement error. It did, however, tend to overpredict changes in slope and underpredict changes in grain size with reductions in sediment supply (Figures 3 and 4). Of course, since the model includes a sediment feed at the furthest upstream node, if run to equilibrium it has to eventually calculate sediment flux everywhere to be equal to the feed rate. So, a robust evaluation of the model's performance must look at the accuracy of its predictions of equilibrium bed states (slope and grain size) and transient conditions.

[32] The surface-based bed load transport relations used in the modeling [*Parker*, 1990; *Wilcock and Crowe*, 2003] calculate sediment flux as a highly nonlinear function of the grain size distribution of the bed surface and the applied shear stress. We can illustrate the relative influence of changes in the bed surface grain size distribution versus changes in shear stress by calculating sediment transport rates under a wide variety of shear stresses and bed surface
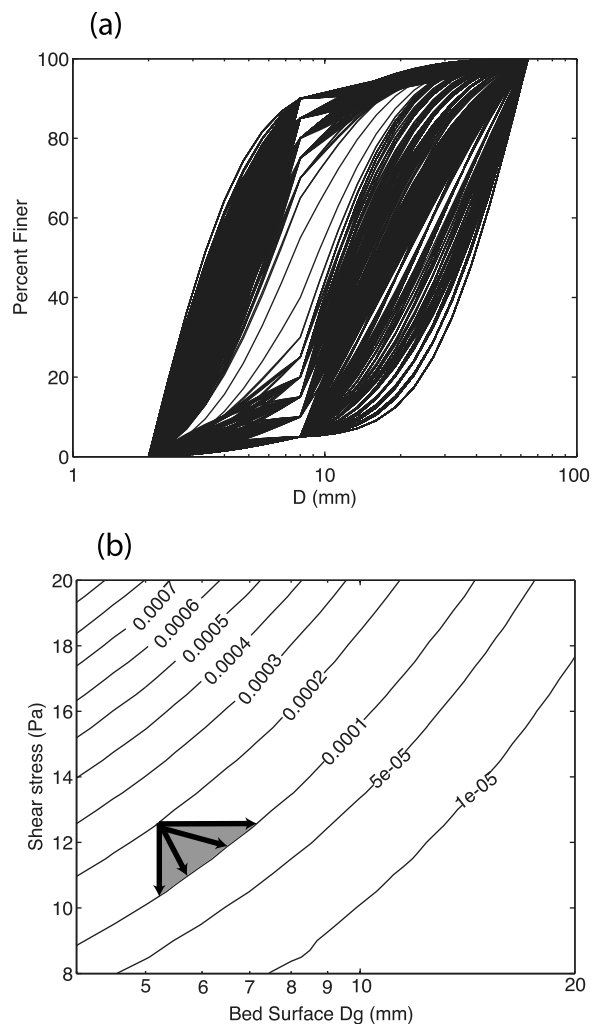
Figure 12. (a) Theoretical bed surface grain size distributions (n = 13071) with varying geometric mean diameters (Dg) but constant geometric standard deviation (σ = 1.9). (b) Contours of constant sediment transport rate (in m²/s) calculated with the algorithm of *Parker* [1990] for the bed surface grain size distributions in Figure 12a and plotted as a function of shear stress and bed surface geometric mean diameter (Dg). The shaded region and arrows represents the region of possible morphodynamic change likely to result from a reduction in sediment supply from 0.0002 to 0.0001 m²/s.

ters in the bed load flux algorithm. The transition from one sediment transport rate to another can be accommodated through a pure grain size change, a pure shear stress change (which, for a constant water discharge is likely to manifest itself by changes primarily in slope rather than in depth), or some combination of change in both variables. The shaded area in Figure 12 illustrates the potential changes in grain size and shear stress that might accompany a flux change from 0.0002 to 0.0001 m²/s, if we assume that supply reductions will inevitably be accompanied by net scour, which can reduce the slope or increase the surface grain size. The precise path taken in response to a supply reduction calculated in a 1-D morphodynamic model will be constrained by the conservation of each grain size and depends on the grain size distribution of the feed. The nonlinear nature of sediment transport calculations is readily apparent; a 100% change in sediment flux can result from a 40% change in Dg or a 15% change in shear stress. Thus, relatively small changes in slope or grain size can produce large changes in calculated sediment flux, and inversely, large changes in sediment flux (or sediment supply) will result in calculated slope or grain size changes that fall within a relatively narrow range.

[33] In field application, estimates of boundary shear stress (from channel slope and flow depth) and surface grain size distribution are commonly used in bed load transport equations to calculate sediment flux. However, such predictions may be problematic in patchy channels, as several authors [e.g., *Paola and Seal*, 1995; *Ferguson*, 2003] have argued that 1-D width-averaged bed load transport calculations tend to underestimate flux if there is cross-stream variance in shear stress that is not exactly compensated by matching changes in grain size. We applied the *Parker* [1990] and *Wilcock and Crowe* [2003] bed load relations to our observed areally averaged bed surface grain size distributions and shear stresses (Figure 13). For the three sediment-feed portions of the Berkeley experiment, the *Parker* [1990] algorithm predicted sediment transport rates within the range of uncertainty. It did overpredict the sediment flux for the zero feed case, suggesting that at very low transport rates the model's underlying calibration breaks down. The *Wilcock and Crowe* [2003] model, applied to both experiments, exhibits contradictory behavior; it tends to underpredict transport rates for the Berkeley experiment and it tends to overpredict transport rates for the Tsukuba experiment. Given this seemingly inconsistent behavior, we are unable to assign a simple mechanism for its inaccuracy (such as overall underprediction due to lateral patchiness, for instance), but the calculations suggest that our experimental conditions may fall outside the realm of the model's applicability. Nonetheless, the rather good performance of the *Parker* [1990] model when applied to the Berkeley experiments suggests that, at least for simple, flume-like conditions, spatial averaging may produce reasonable transport calculations. However, natural gravel beds commonly show greater differences in grain size distributions than observed in our experiments [e.g., *Lisle et al.*, 2000], and one could speculate that for a sinuous channel with larger spatial stress gradients and a wider range of grain sizes spatial averaging may not be sufficient to achieve accurate calculations.
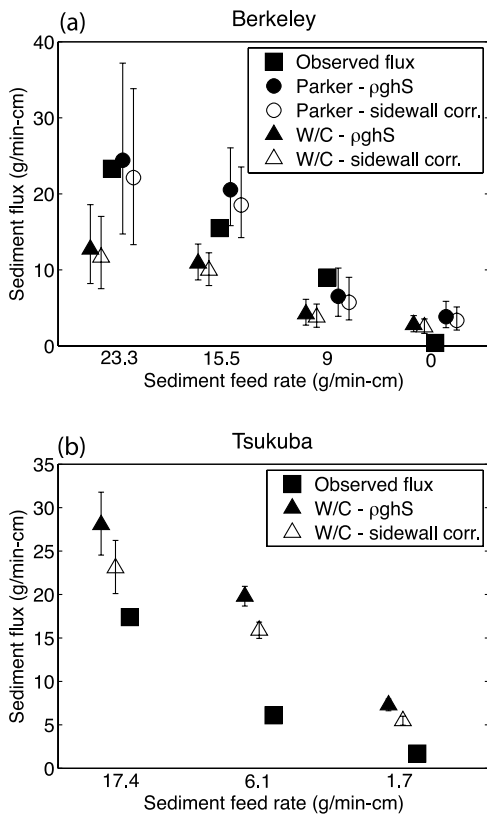
grain size distributions. Figure 12b presents contours of constant sediment transport rate (in m²/s) predicted using the *Parker* [1990] algorithm under varying shear stress for 13,071 theoretical bed surface grain size distributions (Figure 12a) composed of 2–64 mm material that have varying geometric mean diameters (Dg) but constant geometric standard deviation (σ = 1.9). The *Parker* [1990] algorithm uses a straining parameter which is a function of σ, so to isolate the effect of changing Dg we only used grain size distributions with σ = 1.9. Although this results in a population of surface grain size distributions with varying skewness and kurtosis, the impact of this should be minor because higher moments are not used to calculate parame-

Figure 13. Sediment transport rates observed and predicted by the *Parker* [1990] and *Wilcock and Crowe* [2003] models when provided with the experimentally observed areally averaged bed surface grain size distribution (Figure 1) and shear stress. Error bars indicate uncertainty associated with the standard error of the shear stress. Sidewall corrected stresses were calculated with the *Williams* [1970] method.

[34] To examine just the effect of cross-stream variability in grain size compared to using an areally weighted average bed surface grain size distribution in the Parker (e-book, 2007) model, we performed simple calculations in which the channel in each experiment was assumed to be composed of two patch types, the inactive and smooth types (grain size distributions given in Figure 2), with the relative proportion of each patch type varying from 0 to 100% of the channel width. For each bed state, we then used the *Parker* [1990] or *Wilcock and Crowe* [2003] algorithm to calculate the total bed load transport rate for the following two conditions under the same shear stress: (1) the "actual" case where the transport rate is calculated for each grain size distribution and multiplied by its relative proportion across the bed (a "width-integrated" calculation) and (2) the 1-D case where an areally averaged grain size distribution is calculated from the proportions of the two patch types and the algorithm is then used to compute the flux rate over that bed state (a width-averaged calculation). We assume constant shear stress across the channel typical of our experiments: 4.5 Pa for the Tsukuba case and 10 Pa for the Berkeley case. These calculations are the same for the end-member cases of either 100% smooth or 100% inactive or congested

(Figure 14). As the bed transitions from 100% smooth to 100% inactive, the calculated sediment transport rate decreases by about 50% for the Berkeley case and about 70% for the Tsukuba case. The difference between the 2-patch calculation and the 1-D average calculation is at most about 5%. In the Berkeley case, the flux calculated in the width-averaged calculation is always lower than in the width-integrated calculation, which is consistent with previous work [e.g., *Paola and Seal*, 1995; *Ferguson*, 2003]. In the Tsukuba case, however, the width-averaged calculation predicts a higher flux than the width-integrated calculation when the bed is about 80–100% inactive because, for those conditions, the sand content of the average bed grain size distribution increases and thus decreases the critical shear stress through the *Wilcock and Crowe* [2003] sand mobilization parameter. The relatively small effect of grain size
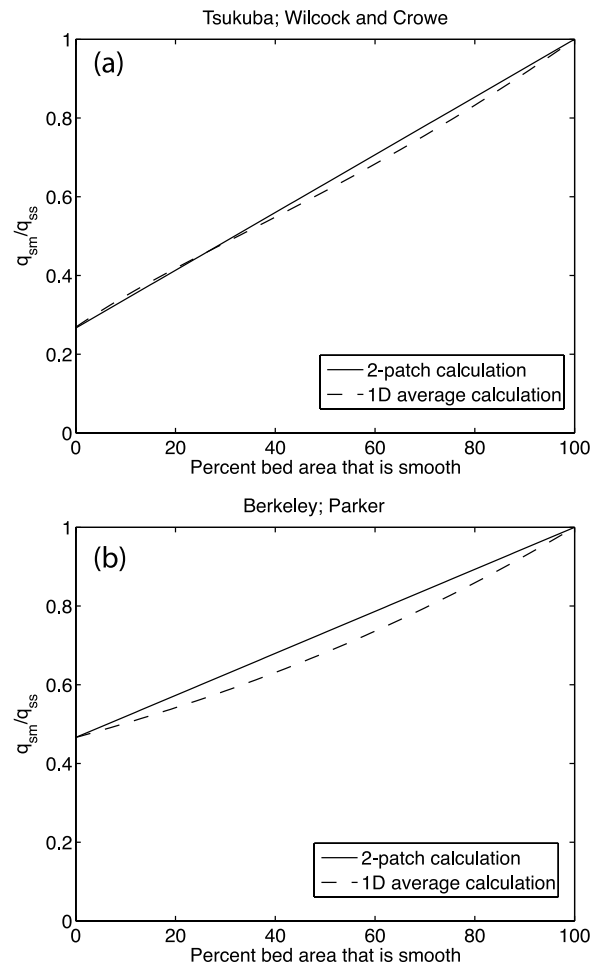

Figure 14. (a) Ratio of sediment flux calculated for a shear stress of 4.5 Pa using the *Wilcock and Crowe* [2003] algorithm for a channel composed of a combination of the Tsukuba "smooth" and "inactive" patch types (q_{sm}) (see Figure 2a for grain size distributions) to that calculated for a 100% smooth channel (q_{ss}). (b) The same information as in Figure 14a except it uses the *Parker* [1990] model to calculate sediment transport under 10 Pa shear stress on a bed that is a mixture of the Berkeley smooth and inactive patch types (see Figure 2b for grain size distributions).

variation alone heightens the importance of spatial variation in the boundary shear stress (relative to surface patch texture). For example, under the spatially constant stress conditions, the flux for the 100% inactive beds was 25–50% of that for the 100% smooth bed, whereas our observations suggested that this ratio should be close to zero (i.e., the bed was truly inactive and no transport should have been predicted). Again, this disparity is probably due to the local low-boundary shear stress over the coarsened near-wall patches. Hence, the results shown in Figure 14 underestimate the combined effect of boundary shear stress and grain size variation.

[35] While the 1-D Parker (e-book, 2007) model was generally able to predict the mean sediment transport rate for both experiments (Figure 11), it was unable to capture the significant short-term variability in sediment flux associated with the passage of individual bed load sheets (Figures 8, 11, and 12). Variations in bed load transport rates are very commonly observed in both field and flume studies [e.g., *Carey*, 1985; *Iseya and Ikeda*, 1987; *Kuhnle and Southard*, 1988; *Whiting et al.*, 1988; *Gomez et al.*, 1989; *Ashmore*, 1991a, 1991b; *Hoey*, 1992; *Lisle et al.*, 1993; *Cudden and Hoey*, 2003; *Bunte and Abt*, 2005; *Whitaker and Potts*, 2007; *Madej et al.*, 2009]. The discrepancy with the model may be a consequence of its simplified hydraulics (the normal flow approximation), or smoothing effects related to the use of upwinding coefficients to calculate spatial derivatives or mixing with the subsurface. The incorporation of more complicated hydrodynamics [e.g., *Seminara et al.*, 1996] or particle-based modeling [e.g., *Schmeeckle and Nelson*, 2003; *MacVicar et al.*, 2006] appears to be necessary to capture this variability. Bed load sheets are an inherent feature of gravel bed channels, and understanding their dynamics is critical to improving bed load flux models.

5. Conclusions

[36] Bed surface patches are a fundamental feature of channels with mixed size sediment. In our experiments, even in the simplest possible case of a straight, low width-to-depth ratio channel with no bed topography subject to constant discharge, the bed became organized into patches of similar grain size and sorting. Freely migrating patches, bed load sheets, formed in both a bimodal sand-gravel mixture and a unimodal sand-free sediment mixture. The primary mechanism of formation and migration of these patches was grain-to-grain interaction via the catch and mobilize process, even in experiments using unimodal, sand-free sediment, which suggests that the ratio of grain diameters, rather than the presence of sand, determines a mobilization feedback. The passage of bed load sheets coincides with substantial increases in sediment flux, suggesting that the migration of free patches can be a primary cause of short-term fluctuations in sediment transport rate commonly observed in rivers and flumes.

[37] Sediment supply controls the relative abundance of fixed and free patches and determines the scaling and dynamics of bed load sheets. In both of our experiments, reductions in sediment supply led to an expansion of coarse patches at the expense of finer ones and a narrowing of

the corridor through which nearly all bed load transport occurred. Reduced sediment supply led to a decrease in sheet migration rate and an increase in the spacing between sheets. Complete elimination of sediment supply resulted in a nearly total loss of bed surface heterogeneity, a uniformly coarse bed and elimination of bed load sheets.

[38] The 1-D Parker (e-book, 2007) morphodynamic model calculated the surface grain size and slope so that it was able to predict the average sediment transport accurately (although short-term fluctuations associated with sheet migration were beyond its capability). Because of the nonlinear relationship between stress, grain size, and sediment transport, the magnitudes of the model's over- or underpredictions of slope and grain size were not severe. The model performed best in low-supply conditions where bed surface patchiness was minimized.

[39] Our experiments demonstrate that bed surface patchiness is tied to sediment supply, as patch abundance and the spatial extent of fine bed material increased with increasing supply. It remains challenging to apply 1-D models to spatially variable beds using current transport equations. Calculations for our simple experimental conditions suggest that the use of areally averaged surface grain size may produce reasonable transport predictions, although it is unclear whether averaging would work in a more complicated field scenario. Our experimental results support the idea that bed patchiness conveys information about the sediment supply in a system, and should be an important feature to document in sediment transport studies.

Notation

D	grain size [L].
$D16, D50, D84$	grain size for which 16, 50, and 84%, respectively, of the grain size distribution is finer [L].
Dg	geometric mean grain size [L].
dt	time step [T].
g	gravitational acceleration [L T^{-2}].
h	water depth [L].
H	bed form height [L].
I	intermittency [dimensionless].
L	bed form length [L].
L_r	reach length [L].
M	number of model segments [dimensionless].
n_a	active layer factor [dimensionless].
p	bed form period [T].
$qbTf$	sediment feed rate [L^2 T^{-1}].
q_s	sediment flux per unit width [M L^{-1} T^{-1}].
q_{sm}	sediment transport calculated for a mixture of smooth and inactive or congested patch types [L^2 T^{-1}].
q_{ss}	sediment transport calculated for a 100% smooth bed [L^2 T^{-1}].
q_w	water discharge [L^2 T^{-1}].
$SfbI$	initial slope [dimensionless].
U	bed form migration rate [L T^{-1}].
ρ	water density [M L^{-3}].

σ geometric standard deviation [dimensionless].

τ_b boundary shear stress [M L^{-2} T^{-2}].

References

Antonia, R. A., and R. E. Luxton (1971), The response of a turbulent boundary layer to a step change in surface roughness. Part 1. Smooth-to-rough, *J. Fluid Mech.*, 48, 721–761, doi:10.1017/S0022112071001824.

Antonia, R. A., and R. E. Luxton (1972), The response of a turbulent boundary layer to a step change in surface roughness. Part 2. Rough-to-smooth, *J. Fluid Mech.*, 53, 737–757, doi:10.1017/S002211207200045X.

Arnott, R. W., and M. Hand (1989), Bedforms, primary structures, and grain fabric in the presence of suspended sediment rain, *J. Sediment. Petrol.*, 59, 1062–1069.

Ashmore, P. (1991a), Channel morphology and bed load pulses in braided, gravel-bed streams, *Geogr. Ann.*, 73, 37–52, doi:10.2307/521212.

Ashmore, P. E. (1991b), How do gravel-bed rivers braid?, *Can. J. Earth Sci.*, 28, 326–341.

Ashworth, P. J., R. I. Ferguson, and M. D. Powell (1992a), Bedload transport and sorting in braided channels, in *Dynamics of Gravel-Bed Rivers*, edited by P. Billi et al., pp. 497–513, John Wiley, Chichester, U. K.

Ashworth, P. J., R. I. Ferguson, P. E. Ashmore, C. Paola, M. D. Powell, and K. L. Prestegaard (1992b), Measurements in a braided river chute and lobe: 2. Sorting of bed load during entrainment, transport, and deposition, *Water Resour. Res.*, 28, 1887–1896, doi:10.1029/92WR00702.

Bennett, S. J., and J. S. Bridge (1995), The geometry and dynamics of low-relief bed forms in heterogeneous sediment in a laboratory channel, and their relationship to water flow and sediment transport, *J. Sediment. Res.*, 65, 29–39.

Best, J. L. (1996), The fluid dynamics of small-scale alluvial bedforms, in *Advances in Fluvial Dynamics and Stratigraphy*, edited by P. A. Carling and M. R. Dawson, pp. 67–125, John Wiley, Chichester, U. K.

Bridge, J. S. (1992), A revised model for water flow, sediment transport, bed topography, and grain size sorting in natural river bends, *Water Resour. Res.*, 28, 999–1013, doi:10.1029/91WR03088.

Buffington, J. M., and D. R. Montgomery (1999a), A procedure for classifying textural facies in gravel-bed rivers, *Water Resour. Res.*, 35, 1903–1914, doi:10.1029/1999WR900041.

Buffington, J. M., and D. R. Montgomery (1999b), Effects of hydraulic roughness on surface textures of gravel-bed rivers, *Water Resour. Res.*, 35, 3507–3521, doi:10.1029/1999WR900138.

Buffington, J. M., and D. R. Montgomery (1999c), Effects of sediment supply on surface textures of gravel bed rivers, *Water Resour. Res.*, 35, 3523–3530, doi:10.1029/1999WR900232.

Bunte, K., and S. R. Abt (2001), Sampling surface and subsurface particle-size distributions in wadable gravel- and cobble-bed streams for analyses in sediment transport, hydraulics, and streambed monitoring, *Tech. Rep. RMRS-GTR-74*, 450 pp., U. S. Forest Service, Fort Collins, Colo.

Bunte, K., and S. R. Abt (2005), Effect of sampling time on measured gravel bed transport rates in a course-bedded stream, *Water Resour. Res.*, 41, W11405, doi:10.1029/2004WR003880.

Bunte, K., S. R. Abt, J. P. Potyondy, and S. E. Ryan (2004), Measurement of coarse gravel and cobble transport using portable bedload traps, *J. Hydraul. Eng.*, 130, 879–893, doi:10.1061/(ASCE)0733-9429(2004)130:9(879).

Carey, W. P. (1985), Variability in measured bedload-transport rates, *Water Resour. Bull.*, 21, 39–48.

Carling, P. A. (1999), Subaqueous gravel dunes, *J. Sediment. Res.*, 69, 534–545.

Chen, L., and M. C. Stone (2008), Influence of bed material size heterogeneity on bedload transport uncertainty, *Water Resour. Res.*, 44, W01405, doi:10.1029/2006WR005483.

Church, M., M. A. Hassan, and J. F. Wolcott (1998), Stabilizing self-organized structures in gravel-bed stream channels: Field and experimental observations, *Water Resour. Res.*, 34, 3169–3179, doi:10.1029/98WR00484.

Clayton, J. A., and J. Pitlick (2008), Persistence of the surface texture of a gravel-bed river during a large flood, *Earth Surf. Processes Landforms*, 33, 661–673, doi:10.1002/esp.1567.

Crowder, D. W., and P. Diplas (1997), Sampling heterogeneous deposits in gravel-bed streams, *J. Hydraul. Eng.*, 123, 1106–1117, doi:10.1061/(ASCE)0733-9429(1997)123:12(1106).

Cudden, J. R., and T. B. Hoey (2003), The causes of bedload pulses in a gravel channel: The implications of bedload grain-size distributions, *Earth Surf. Processes Landforms*, 28, 1411–1428, doi:10.1002/esp.521.

Dietrich, W. E., and J. D. Smith (1984), Bed load transport in a river meander, *Water Resour. Res.*, 20, 1355–1380, doi:10.1029/WR020i010p01355.

Dietrich, W. E., J. W. Kirchner, H. Ikeda, and F. Iseya (1989), Sediment supply and the development of the coarse surface layer in gravel-bedded rivers, *Nature*, 340, 215–217, doi:10.1038/340215a0.

Dietrich, W. E., P. A. Nelson, E. Yager, J. G. Venditti, M. P. Lamb, and L. Collins (2005), Sediment patches, sediment supply, and channel morphology, in *River, Coastal and Estuarine Morphodynamics: RCEM 2005*, edited by G. Parker and M. H. Garcia, pp. 79–90, Taylor and Francis, London.

Dinehart, R. L. (1992), Evolution of coarse gravel bed forms: Field measurements at flood stage, *Water Resour. Res.*, 28, 2667–2689, doi:10.1029/92WR01357.

Ferguson, R. I. (2003), The missing dimension: Effects of lateral variation on 1-D calculations of fluvial bedload transport, *Geomorphology*, 56, 1–14, doi:10.1016/S0169-555X(03)00042-4.

Ferguson, R. I., K. L. Prestegaard, and P. J. Ashworth (1989), Influence of sand on hydraulics and gravel transport in a braided gravel bed river, *Water Resour. Res.*, 25, 635–643, doi:10.1029/WR025i004p00635.

Garcia, C., J. B. Laronne, and M. Sala (1999), Variable source areas of bedload in a gravel-bed stream, *J. Sediment. Res.*, 69, 27–31.

Garcia, C., H. Coen, I. Reid, A. Rovira, X. Úbeda, and J. B. Laronne (2007), Process of initiation of motion leading to bedload transport in gravel-bed rivers, *Geophys. Res. Lett.*, 34, L06403, doi:10.1029/2006GL028865.

Gomez, B., R. L. Naff, and D. W. Hubbell (1989), Temporal variations in bedload transport rates associated with the migration of bedforms, *Earth Surf. Processes Landforms*, 14, 135–156, doi:10.1002/esp.3290140205.

Gran, K. B., D. R. Montgomery, and D. G. Sutherland (2006), Channel bed evolution and sediment transport under declining sand inputs, *Water Resour. Res.*, 42, W10407, doi:10.1029/2005WR004306.

Gustavson, T. C. (1978), Bed forms and stratification types of modern gravel meander lobes, Nueces River, Texas, *Sedimentology*, 25, 401–426, doi:10.1111/j.1365-3091.1978.tb00319.x.

Haschenburger, J. K., and S. P. Rice (2004), Changes in woody debris and bed material texture in a gravel-bed channel, *Geomorphology*, 60, 241–267, doi:10.1016/j.geomorph.2003.08.003.

Hassan, M. A., and M. Church (2000), Experiments on surface structure and partial sediment transport on a gravel bed, *Water Resour. Res.*, 36, 1885–1895, doi:10.1029/2000WR900055.

Hoey, T. (1992), Temporal variations in bedload transport rates and sediment storage in gravel-bed rivers, *Prog. Phys. Geogr.*, 16, 319–338, doi:10.1177/030913339201600303.

Iseya, F., and H. Ikeda (1987), Pulsations in bedload transport rates induced by a longitudinal sediment sorting: A flume study using sand and gravel mixtures, *Geogr. Ann.*, 69, 15–27, doi:10.2307/521363.

Julien, P. Y., and D. J. Anthony (2002), Bed load motion and grain sorting in a meandering stream, *J. Hydraul. Res.*, 40(2), 125–133.

Kinerson, D. (1990), Surface response to sediment supply, M S. thesis, Univ. of Calif., Berkeley, Calif.

Kirchner, J. W., W. E. Dietrich, F. Iseya, and H. Ikeda (1990), The variability of critical shear stress, friction angle, and grain protrusion in water-worked sediments, *Sedimentology*, 37, 647–672, doi:10.1111/j.1365-3091.1990.tb00627.x.

Kleinhans, M. G., A. W. E. Wilbers, A. De Swaff, and J. H. Van Den Berg (2002), Sediment supply limited bedforms in sand-gravel bed rivers, *J. Sediment. Res.*, 72, 629–640, doi:10.1306/030702720629.

Kuhnle, R. A., and J. B. Southard (1988), Bed load transport fluctuations in a gravel bed laboratory channel, *Water Resour. Res.*, 24, 247–260, doi:10.1029/WR024i002p00247.

Kuhnle, R. A., J. K. Horton, S. J. Bennett, and J. L. Best (2006), Bed forms in bimodal sand-gravel sediments: Laboratory and field analysis, *Sedimentology*, 53, 631–654, doi:10.1111/j.1365-3091.2005.00765.x.

Laronne, J. B., and M. J. Duncan (1992), Bedload transport paths and gravel bar formation, in *Dynamics of Gravel-Bed Rivers*, edited by P. Billi et al., pp. 177–202, John Wiley, Chichester, U. K.

Laronne, J. B., C. Garcia, and I. Reid (2001), Mobility of patch sediment in gravel bed streams: Patch character and its implications for bedload, in *Gravel-Bed Rivers V*, edited by M. P. Mosley, pp. 249–290, N. Z. Hydrol. Soc., Wellington.

Lisle, T. E., and S. Hilton (1999), Fine bed material in pools of natural gravel bed channels, *Water Resour. Res.*, 35, 1291–1304, doi:10.1029/1998WR900088.

Lisle, T. E., and M. A. Madej (1992), Spatial variation in armouring in a channel with variable sediment supply, in *Dynamics of Gravel-Bed Rivers*, edited by P. Billi et al., pp. 277–293, John Wiley, Chichester, U. K.

Lisle, T. E., F. Iseya, and H. Ikeda (1993), Response of a channel with alternate bars to a decrease in supply of mixed-size bed load: A flume experiment, *Water Resour. Res.*, 29, 3623–3629, doi:10.1029/93WR01673.

Lisle, T. E., J. M. Nelson, J. Pitlick, M. A. Madej, and B. L. Barkett (2000), Variability of bed mobility in natural, gravel-bed channels and adjustments to sediment load at local and reach scales, *Water Resour. Res.*, 36, 3743–3755, doi:10.1029/2000WR900238.

Lunt, I. A., and J. S. Bridge (2007), Formation and preservation of open-framework gravel strata in unidirectional flows, *Sedimentology*, 54, 71–87, doi:10.1111/j.1365-3091.2006.00829.x.

MacVicar, B. J., L. Parrott, and A. G. Roy (2006), A two-dimensional discrete particle model of gravel bed river systems, *J. Geophys. Res.*, 111, F03009, doi:10.1029/2005JF000316.

Madej, M. A., D. G. Sutherland, T. E. Lisle, and B. Pryor (2009), Channel responses to varying sediment input: A flume experiment modeled after Redwood Creek, California, *Geomorphology*, 103(4), 507–519, doi:10.1016/j.geomorph.2008.07.017.

Mikoš, M., G. Pender, T. Hoey, A. Shvidchenko, and G. Petkovsek (2003), Numerical simulation of graded sediment transport, *Water Mar. Eng.*, 156, 47–51, doi:10.1680/maen.156.1.47.37949.

Mosley, M. P., and D. S. Tindale (1985), Sediment variability and bed material sampling in gravel-bed rivers, *Earth Surf. Processes Landforms*, 10, 465–482, doi:10.1002/esp.3290100506.

Nelson, P. A., J. G. Venditti, and W. E. Dietrich (2005), Response of bed surface patchiness to reductions in sediment supply, *Eos Trans. AGU*, 86(52), Fall Meet. Suppl., Abstract H51H–04.

Paola, C., and R. Seal (1995), Grain size patchiness as a cause of selective deposition and downstream fining, *Water Resour. Res.*, 31, 1395–1407, doi:10.1029/94WR02975.

Parker, G. (1990), Surface-based bedload transport relation for gravel rivers, *J. Hydraul. Res.*, 28, 417–436.

Parker, G., and E. D. Andrews (1985), Sorting of bed load sediment by flow in meander bends, *Water Resour. Res.*, 21, 1361–1373, doi:10.1029/WR021i009p01361.

Parker, G., and P. C. Klingeman (1982), On why gravel bed streams are paved, *Water Resour. Res.*, 18, 1409–1423, doi:10.1029/WR018i005p01409.

Pender, G., and A. Shvidchenko (1999), The observation of bedload sheets in laboratory experiments, paper presented at 28th Congress of the International Association for Hydraulic Research, Int. Assoc. for the Hydraul. Res., Graz, Austria.

Sambrook Smith, G. H., and A. P. Nicholas (2005), Effect on flow structure of sand deposition on a gravel bed: Results from a two-dimensional flume experiment, *Water Resour. Res.*, 41, W10405, doi:10.1029/2004WR003817.

Schmeeckle, M. W., and J. M. Nelson (2003), Direct numerical simulation of bedload transport using a local, dynamic boundary condition, *Sedimentology*, 50, 279–301, doi:10.1046/j.1365-3091.2003.00555.x.

Seal, R., and C. Paola (1995), Observations of downstream fining on the North Fork Toutle River near Mount St. Helens, Washington, *Water Resour. Res.*, 31, 1409–1419, doi:10.1029/94WR02976.

Seminara, G. (1998), Stability and morphodynamics, *Meccanica*, 33, 59–99, doi:10.1023/A:1004225516566.

Seminara, G., M. Colombini, and G. Parker (1996), Nearly pure sorting waves and formation of bedload sheets, *J. Fluid Mech.*, 312, 253–278, doi:10.1017/S0022112096001991.

Simons, D. E., E. V. Richardson, and C. F. Nordin (1965), Bedload equation for ripples and dunes, *U.S. Geol. Surv. Prof. Pap.*, 462-H, 1–9.

Sun, T., P. Meakin, and T. Jøssang (2001a), A computer model for meandering rivers with multiple bedload sizes: 1. Theory, *Water Resour. Res.*, 37, 2227–2241, doi:10.1029/2000WR900396.

Sun, T., P. Meakin, and T. Jøssang (2001b), A computer model for meandering rivers with multiple bedload sizes: 2. Computer simulations, *Water Resour. Res.*, 37, 2243–2258, doi:10.1029/2000WR900397.

Tsujimoto, T. (1990), Instability of longitudinal distribution of fluvial bed-surface composition, *J. Hydrosci. Hydraul. Eng.*, 7, 69–80.

Venditti, J. G., M. Church, and S. J. Bennett (2005), Morphodynamics of small-scale superimposed sand waves over migrating dune bed forms, *Water Resour. Res.*, 41, W10423, doi:10.1029/2004WR003461.

Whitaker, A. C., and D. F. Potts (2007), Coarse bed load transport in an alluvial gravel bed stream, Dupuyer Creek, Montana, *Earth Surf. Processes Landforms*, 32, 1984–2004, doi:10.1002/esp.1512.

Whiting, P. J. (1996), Sediment sorting over bed topography, in *Advances in Fluvial Dynamics and Stratigraphy*, edited by P. A. Carling and M. R. Dawson, pp. 203–228, John Wiley, Chichester, U. K.

Whiting, P. J., W. E. Dietrich, L. B. Leopold, T. G. Drake, and R. L. Shreve (1988), Bedload sheets in heterogeneous sediment, *Geology*, 16, 105–108, doi:10.1130/0091-7613(1988)016<0105:BSIHS>2.3.CO;2.

Wilcock, P. R. (1992), Experimental investigation of the effect of mixture properties on transport dynamics, in *Dynamics of Gravel-Bed Rivers*, edited by P. Billi et al., pp. 109–139, John Wiley, Chichester, U. K.

Wilcock, P. R. (1998), Two-fraction model of initial sediment motion in gravel-bed rivers, *Science*, 280, 410–412, doi:10.1126/science.280.5362.410.

Wilcock, P. R., and J. C. Crowe (2003), Surface-based transport model for mixed size sediment, *J. Hydraul. Eng.*, 129, 120–128, doi:10.1061/(ASCE)0733-9429(2003)129:2(120).

Wilcock, P. R., and S. T. Kenworthy (2002), A two-fraction model for the transport of sand/gravel mixtures, *Water Resour. Res.*, 38(10), 1194, doi:10.1029/2001WR000684.

Wilcock, P. R., S. T. Kenworthy, and J. C. Crowe (2001), Experimental study of the transport of mixed sand and gravel, *Water Resour. Res.*, 37, 3349–3358, doi:10.1029/2001WR000683.

Williams, G. P. (1970), Flume width and water depth effects in sediment transport experiments, *U. S. Geol. Surv. Prof. Pap.*, 562-H, 1–37.

Wolman, M. G. (1954), A method of sampling coarse river bed material, *Eos Trans. AGU*, 35(6), 951–956.

Yager, E. M. (2007), Prediction of sediment transport in steep, rough streams, Ph.D. thesis, Univ. of Calif., Berkeley, Calif.

Yager, E., W. E. Dietrich, J. W. Kirchner, and B. W. McArdell (2005), Prediction of sediment transport and patch dynamics in a steep, rough stream, *Eos Trans. AGU*, 86(52), Fall Meet. Suppl., Abstract H51H–03.

Yager, E. M., J. W. Kirchner, and W. E. Dietrich (2007), Calculating bed load transport in steep boulder bed channels, *Water Resour. Res.*, 43, W07418, doi:10.1029/2006WR005432.

———————————

W. E. Dietrich, J. W. Kirchner, and P. A. Nelson, Department of Earth and Planetary Science, University of California, 307 McCone Hall, Berkeley, CA 94720-4767, USA. (pnelson@berkeley.edu)

H. Ikeda, Environmental Research Center, Tsukuba University, 1-1-1 Tennodai, Tokyo 305-8577, Japan.

F. Iseya, Department of Commercial Science, Jobu University, 634-1 Toyazuka-machi, Gumma 372-8588, Japan.

L. S. Sklar, Department of Geosciences, San Francisco State University, 509 Thornton Hall, 1600 Holloway Avenue, San Francisco, CA 94132, USA.

J. G. Venditti, Department of Geography, Simon Fraser University, 8888 University Drive, Burnaby, BC V5A 1S6, Canada.